

摘 要

标准模型 (SM) 是现代粒子物理的基石, 它可以通过希格斯机制解释质量的产生。中间矢量玻色子 W^\pm 及 Z^0 的发现, 以及它们的质量与标准模型预测的质量非常一致。但是到目前为止, 还没有实验证明希格斯自发对称破缺机制中的质量产生机制, 而且希格斯粒子一直未在实验上被发现。

目前及将来对撞机的一个最主要的任务之一就是研究弱电对称破缺机制以及规范玻色子和费米子的质量起源, 来检测标准模型。目前 TEVATRON, NLC, GLC 等对撞机都在做这方面的努力, 希望能够找到标准模型预言的物理信息及其他信息。

由于轻子对的产生截面可以达到非常高的精度, 而且光子对撞机可以作为正负电子对撞机的一个补充, $\gamma\gamma \rightarrow e^+e^-$ 过程被建议使用。 $\gamma\gamma \rightarrow e^+e^-$ 过程也是一个可能用于对撞机亮度监测的反应道。它可以对对撞机的亮度进行高精度测量。在高性能对撞过程中其弱电单圈辐射修正的贡献可能应当考虑。本文的工作就是计算了 $\gamma\gamma \rightarrow e^+e^-$ 过程在树图及其一圈弱电辐射修正后的反应截面。通过正规化和重整化以及软光子韧致辐射处理, 我们发现紫外发散和红外发散已经被消除了。在最后的結果中, 我们给出了它们的数值结果。我们在 GLC 亮度监测范围内计算了树图的总截面, 以及标准模型下一圈弱电辐射修正后的总截面, 其中包括虚修正和软光子辐射修正。我们还讨论了在 GLC 的亮度监测范围内树图及一圈修正后的总截面随质心能量的变化关系。我们还获得了微分截面与出射电子角度 θ 的关系曲线。最后, 我们得到了每秒钟亮度探测器接收的事例数随对撞能量的变化图以及与出射角度的变化关系图。GLC 的亮度监测范围是 $50\text{mrad} \leq \theta \leq 150\text{mrad}$ 和 $(\pi - 0.15)\text{rad} \leq \theta \leq (\pi - 0.05)\text{rad}$, 其亮度 $L = 10^{34} \text{cm}^{-2}\text{s}^{-1}$ 。我们的理论计算对实验上检验标准模型具有一定的参考价值。

关键词: 标准模型, 弱电辐射修正, 质心能量, 总截面, 微分截面

ABSTRACT

The Standard Model is the basic theory of modern particle physics, which can explain the generation of masses through Higgs Mechanism. The discovery of intermediate vector bosons W^\pm and Z^0 and their masses are highly in accord with the predictions of SM. But by far, there is no experimental phenomenon representing the mass generation mechanism of symmetry breaking mechanism, and the Higgs boson is not found in experiment till now.

One of the most important tasks of colliders is exploring the electroweak symmetry breaking mechanism and the mass generation mechanism of gauge bosons and fermions, which verifying the SM. In the present, efforts are made by TEVATRON, NLC and GLC to find the physical information of the predictions of SM and others.

The process $\gamma\gamma \rightarrow e^+e^-$ has been suggested because the lepton-pair productions cross-section should be known to very high precision and photon collider is a supplement to electron-positron collider. The process $\gamma\gamma \rightarrow e^+e^-$ is a possible channel for luminosity detector of colliders, which can precisely measure the luminosity of colliders. The contribution of one-loop electroweak correction should probably be considered at high-energy collision. In this paper, we calculated the tree-level and one-loop electroweak radiative corrections. After regularization and renormalization and soft-photonic bremsstrahlung radiation, we found that the UV divergence and IR divergence have been removed, and we listed and discussed the numerical results of the removal. We calculated the tree-level integral cross-section and calculated the cross-section with one-loop electroweak corrections to the process $\gamma\gamma \rightarrow e^+e^-$ in the Standard Model (SM), including virtual corrections and soft photon radiative correction. We discussed the relations between the cross-sections in tree level (and one-loop corrected cross sections) and center-mass energy \sqrt{s} in the luminosity measuring ranges of GLC. We also acquired the relation curves between differential cross section and the outgoing electron angle θ . At last, the numbers of events at different center-mass energy and angular ranges are acquired in the end of the numerical calculations. The luminosity monitor ranges of GLC is $50\text{mrad} \leq \theta \leq 150\text{mrad}$ and $(\pi - 0.15)\text{rad} \leq \theta \leq (\pi - 0.05)\text{rad}$ and the luminosity of GLC is $L = 10^{34} \text{cm}^{-2}\text{s}^{-1}$. We

hope our theoretical calculations have somewhat value to test the Standard Model in experiment.

Keywords: Standard Model, electroweak radiative correction, center-mass energy, integral cross-section, differential cross-section

1 Preface

The $SU(3) \times SU(2) \times U(1)$ standard theory^{[1][2][3]} has passed many precision tests during the last years. In particular, measurements of the muon decay constant G_μ , the gauge boson masses M_W and M_Z , and the decay widths and asymmetries of the Z boson at LEP have provided stringent constraints which are successfully fulfilled by the Standard Model (SM) evaluated at one-loop level. The experimental data favor a value for the top-quark mass which is in accordance with the direct measurements^{[4][5]} of CDF, $m_t = 176 \pm 16$ GeV, and DØ, $m_t = 199 \pm 30$ GeV^{[6][7][8]}. Nevertheless, further precision tests of the SM are required. Up to now, only weak direct experimental information exists on the non-Abelian self-interaction of the gauge bosons^[9]. Moreover, no experimental evidence on the mechanism of spontaneous symmetry breaking, which is responsible for mass generation and postulates the existence of the scalar Higgs boson, has been found yet. For such investigations, energies of several hundred GeV or even few TeV are needed, since the sensitivity to deviations from the SM gauge-boson self-interaction grows strongly with energy, and the existence of the Higgs particle can be proven only by direct production. To this end, a "Next Linear Collider" (NLC) for ee , $e\gamma$, and $\gamma\gamma$ collisions was proposed^[10] which offers a unique environment for such precision experiments owing to the comparably small background.

Since the suggestion of a photon linear collider (PLC^{[11][12][13]}) in the 80's^[14] as an additional option for future e^+e^- linear colliders^{[15][16][17][18]}, many studies on the feasibility (see Ref.^[19] and references therein) and the physics potential^{[20][21]} of such a machine have been performed. A PLC provides an excellent device complementary to e^+e^- colliders. Photon-photon collisions allow for a search of Higgs bosons by s-channel production and for high-precision tests of the properties of W bosons, which are produced in pairs with an enormously large cross section. Moreover, the production cross sections of charged particles, in many models for new physics, are even larger than for comparable e^+e^- machines^[22]. Last but not least, a PLC allows various QCD studies, in particular the investigation of the structure of the photon itself.

According to the DESY/ECFA study^[19] a total $\gamma\gamma$ luminosity of 10^{33} cm⁻²s⁻¹, or even 1–2 orders of magnitude higher, can be reached by Compton backscattering of laser photons off the high-energetic e^+ beams at a 500 GeV collider. This production mechanism renders the luminosity spectrum non-trivial, since both photon beams are

not monochromatic, and a luminosity monitor has to be sensitive to both photon energies. For this task the processes $\gamma\gamma \rightarrow e^+e^-$, $\mu^+\mu^-$ have been suggested (see Ref.^[19] and references therein) as reference reactions. Thus, the lepton-pair production cross section should be known to very high precision.

The process $\gamma\gamma \rightarrow e^+e^-$ is a possible channel for luminosity detector of colliders, which can precisely measure the luminosity of colliders. The contribution of one-loop electroweak correction should probably be considered at a high energy collision. In this paper, we will discuss the process $\gamma\gamma \rightarrow e^+e^-$ in detail at the model of SM. We will calculate the tree-level integral cross section and the one-loop electroweak corrected integral cross section and their differential cross sections. After regularization and renormalization, we will find the UV divergence and IR divergence will be removed. In order to connect with experiments, we choose the luminosity detector range $50\text{mrad} \leq \theta \leq 150\text{mrad}$ and $(\pi - 0.15)\text{rad} \leq \theta \leq (\pi - 0.05)\text{rad}$ of GLC^[20]. The process $\gamma\gamma \rightarrow e^+e^-$ has a little practical meaning for luminosity detection of colliders. We hope our calculations can provide somewhat consult for experiments.

This paper is organized as follows: in Section 2 and Section 3 we introduce some theoretical knowledge that our calculations need. In Section 4 we list all of the Feynman rules of the process $\gamma\gamma \rightarrow e^+e^-$ and its one-loop corrections. After that, we draw the Feynman diagrams by using of FeynArts32. The Section 5 is our main work: the calculations of tree-level integral cross-section and one-loop corrected integral cross-section and the calculations of differential cross-sections. The conclusion is given in Section 6. At last, we will give the references and acknowledgements.

2 The Standard Model

2.1 Introduction

All known particle physics phenomena are extremely well described within the Standard Model (SM) of elementary particles and their fundamental interactions. The SM provides a very elegant theoretical framework and it has successfully passed very precise tests that at present are at the 0.1% level^[25]. The elementary particles in Standard Model are shown in Table 2.1.

Table 2.1 the elementary particles in Standard Model

Elementary Particles						
Quarks	u up	c charm	t top	g gluon	Force Carriers	
	d down	s strange	b bottom	γ photon		
Leptons	ν_e e^- neutrino	ν_μ μ^- neutrino	ν_τ τ^- neutrino	W W boson		
	e electron	μ muon	τ tau	Z Z boson		
3 →	I	II	III	←	Generations	

We understand by elementary particles the point-like constituents of matter with no known substructure up to the present limits of $10^{-18} - 10^{-19}$ m. These are of two types, the basic building blocks of matter themselves known as matter particles and the intermediate interaction particles. The first ones are fermions of spin $s = \frac{1}{2}$ and are classified into leptons and quarks. The known leptons are: the electron, e^- , the muon, μ^- and the τ^- with electric charge $Q = -1$ (all charges are given in units of the

elementary charge e); and the corresponding neutrinos ν_e , ν_μ and ν_τ with $Q=0$.

The known quarks are of six different flavors: u , d , s , c , b and t and have fractional charge $Q = \frac{2}{3}$, $Q = -\frac{1}{3}$, $Q = -\frac{1}{3}$, $Q = \frac{2}{3}$, $Q = -\frac{1}{3}$ and $Q = \frac{2}{3}$ respectively.

The quarks have an additional quantum number, the color, which for them can be of three types, generically denoted as $q, i=1,2,3$. We know that color is not seen in Nature and therefore the elementary quarks must be confined into the experimentally observed matter particles, the hadrons. These colorless composite particles are classified into baryons and mesons. The baryons are fermions made of three quarks, qqq , as for instance the proton, $p \sim uud$, and the neutron, $n \sim ddu$. The mesons are bosons made of one quark and one antiquark as for instance the pions, $\pi^+ \sim u\bar{d}$ and $\pi^- \sim \bar{u}d$.

The second kind of elementary particles is the intermediate interaction particle. By leaving apart the gravitational interactions, all the relevant interactions in Particle Physics are known to be mediated by the exchange of an elementary particle that is a boson with spin $s=1$. The photon, γ , is the exchanged particle in the electromagnetic interactions, the eight gluons $g_\alpha; \alpha=1, \dots, 8$ mediate the strong interactions among quarks, and the three weak bosons, W^\pm, Z are the corresponding intermediate bosons of the weak interactions.

As for the theoretical aspects, the SM is a quantum field theory that is based on the gauge symmetry $SU(3)_C \times SU(2)_L \times U(1)_Y$. This gauge group includes the symmetry group of the strong interactions, $SU(3)_C$, and the symmetry group of the electroweak interactions, $SU(2)_L \times U(1)_Y$. The group symmetry of the electromagnetic interactions, $U(1)_{em}$, appears in the SM as a subgroup of $SU(2)_L \times U(1)_Y$ and it is in this sense that the weak and electromagnetic interactions are said to be unified.

The gauge sector of the SM is composed of eight gluons which are the gauge bosons of $SU(3)_C$ and the γ , W^\pm and Z particles which are the four gauge bosons of $SU(2)_L \times U(1)_Y$. The main physical properties of these intermediate gauge bosons are as follows. The gluons are massless, electrically neutral and carry color quantum number. There are eight gluons since they come in eight different colors. The consequence of the gluons being colorful is that they interact not just with the quarks but also with themselves. The weak bosons, W^\pm and Z are massive particles and also selfinteracting. The W^\pm are charged with $Q = \pm 1$ respectively and the Z is electrically neutral. The photon is massless, chargeless and non-selfinteracting. Concerning the range of the

various interactions, it is well known the infinite range of the electromagnetic interactions as it corresponds to an interaction mediated by a massless gauge boson, the short range of the weak interactions of about 10^{-16} cm correspondingly to the exchange of a massive gauge particle with a mass of the order of $M_\nu \sim 100$ GeV and, finally, the strong interactions whose range is not infinite, as it should correspond to the exchange of a massless gluon, but finite due to the extra physical property of confinement. In fact, the short range of the strong interactions of about 10^{-13} cm corresponds to the typical size of the lightest hadrons.

As for the strength of the three interactions, the electromagnetic interactions are governed by the size of the electromagnetic coupling constant e or equivalently $\alpha = \frac{e^2}{4\pi}$ which at low energies is given by the fine structure constant, $\alpha(Q = m_e) = \frac{1}{137}$. The weak interactions at energies much lower than the exchanged gauge boson mass, M_ν , have an effective (weak) strength given by the dimensionful Fermi constant $G_F = 1.167 \times 10^{-5} \text{ GeV}^{-2}$. The name of strong interactions is due to their comparative stronger strength than the other interactions. This strength is governed by the size of the strong coupling constant g_s or equivalently $\alpha_s = \frac{g_s^2}{4\pi}$ and is varies from large values to low energies, $\alpha_s(Q = m_{\text{hadron}}) \sim 1$ up to the vanishing asymptotic limit $\alpha_s(Q \rightarrow \infty) \rightarrow 0$. This last limit indicates that the quarks behave as free particles when they are observed at infinitely large energies or, equivalently, infinitely short distances and it is known as the property of asymptotic freedom.

The fermionic sector of quarks and leptons are organized in three families with identical properties except for mass. The particle content in each family is:

$$1^{\text{st}} \text{ family: } \begin{pmatrix} \nu_e \\ e^- \end{pmatrix}_L, e_R^-, \begin{pmatrix} u \\ d \end{pmatrix}_L, u_R, d_R \quad (2.1)$$

$$2^{\text{nd}} \text{ family: } \begin{pmatrix} \nu_\mu \\ \mu^- \end{pmatrix}_L, \mu_R^-, \begin{pmatrix} c \\ s \end{pmatrix}_L, c_R, s_R \quad (2.2)$$

$$3^{\text{rd}} \text{ family: } \left(\begin{array}{c} \nu_{\tau} \\ \tau^- \end{array} \right)_L, \tau_R^-, \left(\begin{array}{c} t \\ b \end{array} \right)_L, t_R, b_R \quad (2.3)$$

and their corresponding antiparticles. The left-handed and right-handed fields are defined by means of the chirality operator γ_5 as usual

$$e_L^- = \frac{1}{2}(1 - \gamma_5)e^-; e_R^- = \frac{1}{2}(1 + \gamma_5)e^- \quad (2.4)$$

and they transform as doublets and singlets of $SU(2)_L$ respectively.

The scalar sector of the SM is not experimentally confirmed yet. The fact that the weak gauge bosons are massive particles, $M_W^\pm, M_Z \neq 0$, indicates that $SU(2)_L \times U(1)_Y$ is NOT a symmetry of the vacuum. In contrast, the photon being massless reflects that $U(1)_{em}$ is a good symmetry of the vacuum. Therefore, the Spontaneous Symmetry Breaking pattern in the SM must be:

$$SU(1)_C \times SU(2)_L \times U(1)_Y \rightarrow SU(3)_C \times U(1)_{em} \quad (2.5)$$

The above pattern is implemented in the SM by means of the so-called Higgs Mechanism which provides the proper masses to the M^\pm and Z gauge bosons and to the fermions, and leaves as a consequence the prediction of a new particle: The Higgs boson particle. This must be scalar and electrically neutral. This particle has not been seen in the experiments so far^[28].

2.2 Classification of Internal Symmetries and Relevant Theorems

There are two distinct classes of internal symmetries:

A. global symmetries

The continuous parameters of the transformation DO NOT DEPEND on the space-time coordinates. Some examples are: $SU(2)$ Isospin symmetry, $SU(3)$ flavor symmetry, $U(1)_B$ baryon symmetry, $U(1)_L$ lepton symmetry,...

B. local (gauge) symmetries

The continuous parameters of the transformation DO DEPEND on the space-time coordinates. Some examples are: $U(1)_{em}$ electromagnetic symmetry, $SU(2)_L$ weak isospin symmetry, $U(1)_Y$ weak hypercharge symmetry, $SU(3)_C$ color symmetry,...

There are two relevant theorems/principles that apply to the two cases above respectively and have important physical implications:

Noether's Theorem for Global Symmetries

If the Hamiltonian (or the Lagrangian) of a physical system has a global symmetry,

there must be a current and the associated charge that are conserved.

The Gauge Principle for Gauge Theories

Let Ψ be a physical system in Particle Physics whose dynamics is described by a Lagrangian L which is invariant under a global symmetry G . It turns out that, by promoting this global symmetry G from global to local, the originally free theory transforms into an interacting theory. The procedure in order to get the theory invariant under local transformations is by introducing new vector boson fields, the so-called gauge fields, which interact with the Ψ field in a gauge invariant manner. The number of gauge fields and the particular form of these gauge invariant interactions depend on the particularities of the symmetry group G . More specifically, the number of associated gauge boson fields is equal to the number of generators of the symmetry group G .

The above Gauge Principle is a very important aspect of Particle Physics and has played a crucial role in the building of the Standard Model.

The quantum field theories that are based on the existence of some gauge symmetry are called Gauge Theories. We have already mentioned the cases of $U(1)_{em}$, $SU(2)_L$, $U(1)_Y$ and $SU(3)_C$ gauge symmetries. The gauge theory based on $U(1)_{em}$ is Quantum Electrodynamics (QED), the gauge theory based on $SU(3)_C$ is Quantum Chromodynamics (QCD) and the corresponding one based on the composed group $SU(2)_L \times U(1)_Y$ is the so-called Electroweak Theory. The Standard Model is the gauge theory based on the total gauge symmetry of the fundamental interactions in particle physics, $SU(3)_C \times SU(2)_L \times U(1)_Y$.

2.3 Lagrangian of the Electroweak Theory

In order to get the total Lagrangian of the Electroweak Theory one must add to the previous fermion terms containing the kinetic and fermion interaction terms, the gauge boson kinetic terms and the gauge boson self-interaction terms. The SM total Lagrangian can be written as

$$L_{SM} = L_f + L_G + L_{SBS} + L_{\gamma W} \quad (2.6)$$

where the fermion Lagrangian is

$$L_f = \sum_{f=1,2} \bar{f} i \not{D} f \quad (2.7)$$

and the Lagrangian for the gauge fields is

$$L_G = -\frac{1}{4}W'_{\mu\nu}W'^{\mu\nu} - \frac{1}{4}B_{\mu\nu}B^{\mu\nu} + L_{GF} + L_{FP} \quad (2.8)$$

which is written in terms of the field strength tensors

$$W'_{\mu\nu} = \partial_\mu W'_\nu - \partial_\nu W'_\mu + g\varepsilon^{ijk}W'_\mu{}^jW'_\nu{}^k \quad (2.9)$$

$$B_{\mu\nu} = \partial_\mu B_\nu - \partial_\nu B_\mu \quad (2.10)$$

L_{GF} and L_{FP} are the gauge fixing and Faddeev Popov Lagrangians respectively that are needed in any gauge theory. We omit to write them here for brevity. These have also been omitted in the cases of QCD and QED.

Notice that this gauge Lagrangian contains the wanted self-interaction terms among the three $W'_\mu{}^i, i=1,2,3$ gauge bosons, as it corresponds to a non-abelian $SU(2)_L$ group.

The last two terms, L_{SBS} and L_{YW} are the Symmetry Breaking Sector Lagrangian and the Yukawa Lagrangian respectively. These terms are needed in order to provide the wanted M_W and M_Z gauge boson masses and m_f fermion masses.

One can show that L_{SM} is indeed invariant under the following $SU(2)_L \times U(1)_Y$ gauge transformations:

$$f_L \rightarrow e^{i\vec{T}\vec{\theta}(x)} f_L \quad (2.11)$$

$$f \rightarrow e^{i\frac{Y}{2}\alpha(x)} f \quad (2.12)$$

$$f_R \rightarrow f_R \quad (2.13)$$

$$W'_\mu \rightarrow W'_\mu - \frac{1}{g}\partial_\mu\theta^i(x) + \varepsilon^{ijk}\theta^jW'_\mu{}^k \quad (2.14)$$

$$B_\mu \rightarrow B_\mu - \frac{1}{g'}\partial_\mu\alpha(x) \quad (2.15)$$

The physical gauge bosons W_μ^\pm , Z_μ and A_μ are obtained from the electroweak interaction eigenstates by the following expressions

$$W_\mu^\pm = \frac{1}{\sqrt{2}}(W_\mu^1 \mp iW_\mu^2) \quad (2.16)$$

$$Z_\mu = c_w W_\mu^3 - s_w B_\mu \quad (2.17)$$

$$A_\mu = s_w W_\mu^3 + c_w B_\mu \quad (2.18)$$

where, θ_w defines the rotation in the neutral sector. The relations among the various couplings are obtained by identifying the interactions terms with those of L_{int} . Thus one gets

$$g = \frac{e}{s_w}, g' = \frac{e}{c_w} \quad (2.19)$$

Finally, note that mass terms as $M_W^2 W_\mu W^\mu$, $\frac{1}{2} M_Z^2 Z_\mu Z^\mu$ and $m_f \bar{f} f$ are forbidden by $SU(2)_L \times U(1)_Y$ gauge invariance. This is a new situation that is not found in QED or QCD. The needed gauge boson masses must be generated in a gauge invariant way. The spontaneous breaking of the $SU(2)_L \times U(1)_Y$ symmetry and the Higgs Mechanism provide indeed this mass generation. To this subject we come next.

2.4 The Concept of Spontaneous Symmetry Breaking and the Higgs Mechanism

2.4.1 The Concept of Spontaneous Symmetry Breaking (SSB)

One of the key ingredients of the SM of electroweak interactions is the concept of Spontaneous Symmetry Breaking (SSB), giving rise to Goldstone excitations^[29] which in turn can be related to gauge boson mass terms^[28]. When this SSB refers to a gauge symmetry instead of a global symmetry, then the Higgs Mechanism operates^{[32][32]}. This procedure is needed in order to describe the short ranged weak interactions by a gauge theory without spoiling gauge invariance. The discovery of the W^\pm and Z gauge bosons at CERN in 1983^{[37][34][35][36][37]} may be considered as the first experimental evidence of the SSB phenomenon in electroweak interactions. In present and future experiments one hopes to get insight into the nature of this Symmetry Breaking Sector (SBS) and this is one of the main motivations for constructing the next generation of accelerators. In particular, it is the most exciting challenge for the LHC collider being built at CERN.

In the SM, the symmetry breaking is realized linearly by a scalar field which acquires a non-zero vacuum expectation value. The resulting physical spectrum contains

not only the massive intermediate vector bosons and fermionic matter fields but also the Higgs particle, a neutral scalar field which has escaped experimental detection until now. The main advantage of the SM picture of symmetry breaking lies in the fact that an explicit and consistent formulation exists, and any observable can be calculated perturbatively in the Higgs self-coupling constant. However, the fact that one can compute in a model doesn't mean at all that this is the right one.

The concept of spontaneous electroweak symmetry breaking is more general than the way it is usually implemented in the SM. Any alternative SSB has a chance to replace the standard Higgs sector, provided it meets the following basic requirements: 1) Electromagnetism remains unbroken; 2) The full symmetry contains the electroweak gauge symmetry; 3) The symmetry breaking occurs at about the energy scale $v = (\sqrt{2}G_F)^{-\frac{1}{2}} = 246 \text{ GeV}$ with G_F being the Fermi coupling constant. A simple definition of the phenomenon of SSB is as follows:

A physical system has a symmetry that is spontaneously broken if the interactions governing the dynamics of the system possess such a symmetry but the ground state of this system does not.

In the language of Quantum Field Theory, a system is said to possess a symmetry that is spontaneously broken if the Lagrangian describing the dynamics of the system is invariant under these symmetry transformations, but the vacuum of the theory is not. Here the vacuum $|0\rangle$ is the state where the Hamiltonian expectation value $\langle 0|H|0\rangle$ is minimum.

2.4.2 Goldstone Theorem

The general situation in Quantum Field Theory is described by the Goldstone Theorem^[39]

If a Theory has a global symmetry of the Lagrangian which is not a symmetry of the vacuum then there must exist one massless boson, scalar or pseudoscalar, associated to each generator which does not annihilate the vacuum and having its same quantum numbers. These modes are referred to as Nambu-Goldstone bosons or simply as Goldstone bosons.

2.4.3 The Higgs Mechanism

The Goldstone Theorem is for theories with spontaneously broken global symmetries, but does not hold for gauge theories. When a spontaneous symmetry breaking takes place in a gauge theory the so-called Higgs Mechanism operates.

The would-be Goldstone bosons associated to the global symmetry breaking do not

manifest explicitly in the physical spectrum but instead they 'combine' with the massless gauge bosons and as result, once the spectrum of the theory is built up on the asymmetrical vacuum, there appear massive vector particles. The number of vector bosons that acquire a mass is precisely equal to the number of these would-be-Goldstone bosons.

There are three important properties of the Higgs Mechanism for 'mass generation' that are worth mentioning:

- 1.- It respects the gauge symmetry of the Lagrangian.
- 2.- It preserves the total number of polarization degrees.
- 3.- It does not spoil the good high energy properties nor the renormalizability of the massless gauge theories.

We now turn to the case of the SM of Electroweak Interactions. We will see in the following how the Higgs Mechanism is implemented in the $SU(2)_L \times U(1)_Y$ Gauge Theory in order to generate a mass for the weak gauge bosons, W^\pm and Z . The following facts must be considered:

- 1.- The Lagrangian of the SM is gauge $SU(2)_L \times U(1)_Y$ symmetric. Therefore, anything we wish to add must preserve this symmetry.
- 2.- We wish to generate masses for the three gauge bosons W^\pm and Z but not for the photon, γ . Therefore, we need three would-be-Goldstone bosons, ϕ^+, ϕ^- and χ , which will combine with the three massless gauge bosons of the $SU(2)_L \times U(1)_Y$ symmetry.
- 3.- Since $U(1)_{em}$ is a symmetry of the physical spectrum, it must be a symmetry of the vacuum of the Electroweak Theory.

From the above considerations we conclude that in order to implement the Higgs Mechanism in the Electroweak Theory we need to introduce an 'ad hoc' additional system that interacts with the gauge sector in a $SU(2)_L \times U(1)_Y$ gauge invariant manner and whose self-interactions, being also introduced 'ad hoc', must produce the wanted breaking, $SU(2)_L \times U(1)_Y \rightarrow U(1)_{em}$, with the three associated would-be-Goldstone bosons ϕ^+, ϕ^- and χ . This system is the so-called SSB of the Electroweak Theory.

3 Regularization and Renormalization Theory

3.1 Regularization

The goal of regularization is to explicitly calculate the divergent integral:

$$I = \int_0^\infty d^2 k F(k) \quad (3.1)$$

This can be done a number of ways. Furthermore, the end result should not depend on which regularization scheme you chose. The idea will always be to reparametrize the integral in terms of a parameter. After we have expressed the integral in this way, we will take the physical limit where the result returns to the original integral. Terms that vanish, we will ignore. Terms that blow up, we will need to get rid of. The end result will be something finite.

In this section we will present four different regularization schemes. There are many more, but these are probably the most commonly used. Notice that every term in this section can also depend on physical quantities such as mass, charge and external momenta. We are suppressing this dependence, as it is not relevant to the regularization scheme.

Momentum Cutoff. We are evaluating integrals that have the form of Equation (3.1). This integral diverges at the large limit. Then perhaps the most obvious choice for a regularization scheme is not to integrate to infinity, but to a very large momentum, parametrized by the Greek letter Λ :

$$I \rightarrow I_\Lambda \equiv \int_0^\Lambda d^4 k F(k) \quad (3.2)$$

I_Λ is certainly convergent, and becomes I in the limit $\Lambda \rightarrow \infty$. We can do this integral to get the general result:

$$I_\Lambda = A(\Lambda) + B + C\left(\frac{1}{\Lambda}\right) \quad (3.3)$$

where in the physical limit $\Lambda \rightarrow \infty$, A is divergent (either power-law or logarithmically), C vanishes, and B is independent of Λ and hence remains finite. We can immediately drop C , and we are left with a piece that diverges and a piece that is finite. If we can only figure out a way to get rid of the divergent piece, we can take the limit and get a finite answer. This is exactly what we will do in step 2. But before getting there, we'd like to present a few more regularization schemes.

Although momentum cutoff regularization is probably the most obvious choice for a regulator, it is rarely the best one. The reason is that the momentum cutoff dependence almost always violates an important symmetry of the theory such as gauge invariance, which is needed to make sure quantities cancel correctly. Therefore, unless we want a qualitative understanding of the diagram, we almost never use momentum cutoff regularization in practice.

Dimensional Regularization. DimReg, as opposed to momentum cutoff, is one of the most useful and least intuitive regulators. The reason for its usefulness is that it preserves gauge invariance and keeps all the symmetries of the theory manifest.

In DimReg, we replace our integrals with:

$$I \rightarrow I_D = \int_0^\infty d^D k F(k) \quad (3.4)$$

where D is the dimension of our measure. This is NOT to be confused with extra dimensions and string theory - the physical result corresponds to $D=4$. To that end we can perform the integral in D spacetime dimensions, and replace $D \rightarrow 4 - \varepsilon$, so that the physical limit is $\varepsilon \rightarrow 0$. We are left with:

$$I_\varepsilon = A(\varepsilon) + B + C\left(\frac{1}{\varepsilon}\right) \quad (3.5)$$

This time, however, it is A which we can drop immediately in the physical limit. Again, the goal of step 2 will be to find a way to remove the divergent piece, leaving the finite piece over when we take the limit $\varepsilon \rightarrow 0$.

Pauli-Villars Regularization. PV regularization involves the intriguing philosophical assumption that there is more physics going on than we see. When writing down the amplitude, assume that there is another diagram with a loop, this time with a particle of mass M larger than anything else in the theory. However, this diagram enters with the wrong sign! Hence you are subtracting a diagram from your theory. Diagrams with massive loops behave as $\frac{1}{M^2}$, so in the limit $M \rightarrow \infty$ this diagram does not contribute. However, while keeping M finite it will help to cancel divergences. The logic works exactly like momentum cutoff regularization, where we must remove terms that diverge with M and drop terms that vanish in the physical limit, leaving a finite result.

Lattice Regularization. Lattice regularization is a very different beast than the regulators we have been talking about, but we feel obligated to talk about it here because it is truly very beautiful. In lattice regularization, you assume that the universe

is not a continuum, but rather a discrete lattice. Now all of the integrals are actually sums, and you never integrate to infinity since there is a natural cutoff, namely the lattice spacing a . After performing the finite sums, you take your theory off the lattice by going to the physical limit $a \rightarrow 0$. Again, you get terms that diverge with a that you must remove by the renormalization step.

Lattice regularization is very different from any of the other schemes because it is not perturbative. In other words, you use lattice regularization when you are trying to solve a problem without using perturbation theory. This is very useful in theories with the strong force described by quantum chromodynamics (QCD), since the perturbative regime of QCD is very limited. Lattice QCD has been very successful in predicting many results of low-energy QCD, including confinement, hadrons masses and form factors.

3.2 Theory of Renormalization

You might still be bothered by many things in the previous section. When we renormalize physical quantities such as charge and mass, you might be thinking that these quantities are observable and are not infinite. So how can you get away with making them divergent and then ignoring it! The answer to that question is actually deeper than it first seems.

First of all, there is a flaw to the skeptic's argument that the electron is not infinitely massive or carries infinite charge. In fact, according to QFT, it does! The reason we don't see it is subtle but beautiful. If the electron has infinite charge, then it has an infinite amount of energy from the electromagnetic field. This energy manifests itself by the uncertainty principle which says that the field is allowed to create and destroy particles in very short times; such particles are called "virtual particles". With this huge amount of energy, the field is able to produce many particles with charge all around the electron. But because these virtual particles are charged, they line up with the field and dampen the strength, analogously to dielectrics in classical electrodynamics. Hence as you go further away from the electron, its effective charge becomes weaker due to this dielectric effect, thus lowering the charge of the electron to the values we measure.

But in that case, shouldn't the electron's charge get larger and larger as we get closer and closer to it, cutting through this quantum dielectric? The answer is yes, and perhaps even more amazingly, this is precisely what happens! In the everyday world,

we measure $\alpha = \frac{1}{137}$, but at high-energy accelerators such as the Tevatron at Fermilab, we measure $\alpha = \frac{1}{128}$ this is a real effect.

In the past, this effect has been calculated directly by deriving the "Uehling Potential" which is the quantum correction to the Coulomb potential. However, in the past thirty years or so, physicists have developed a much more powerful technique for describing these results in a beautifully elegant and intuitive way. This technique was pioneered by physicists K. Wilson, M. Fisher, L. Kadanoff and others. The technique is called the Renormalization group.

The renormalization group is a very complicated object, but we will just say a few things about it. In general, the idea is to do everything that we have been doing, only now our RC will generally depend on the scale of our experiment; call it μ . This scale is referred to as a subtraction point; its value depends on the scale of the experiment as well as the subtraction scheme. Then we can ask: "How do our physical parameters depend on our subtraction point?" We can write down a set of differential equations, called the "renormalization group equations" that try to answer how our couplings and masses evolve with changing subtraction point. This gives us the results we said above.

It is this technique that has led to the discovery of asymptotic freedom, the key quality of QCD, where the forces get weaker as the subtraction point increases. This allows for a perturbative analysis of QCD at high energies, when perturbation theory fails at low energies. In addition, the renormalization group has helped to solve a number of questions in statistical mechanics, such as the behavior of magnets, liquid crystals and general phase transitions, just to name a few.

The technique of regularization gave us a way to "parameterize the infinities". Now we must develop a way to get rid of these infinities. This is the step of renormalization. For the sake of notation, we will call our regulator Λ ; this does not mean that we have used momentum cutoff regularization.

Up to this point, the integral we have been considering can be denoted the following way:

$$I \equiv I(m, \alpha, \Lambda) \tag{3.6}$$

This quantity blows up in the physical limit. However, it turns out that we can capture this divergence if we make a clever shift of the physical parameters:

$$m \rightarrow m(\Lambda) = m + \delta m(\Lambda) \quad (3.7)$$

$$\alpha \rightarrow \alpha(\Lambda) \equiv \alpha + \delta\alpha(\Lambda) \quad (3.8)$$

$$I(m, \alpha, \Lambda) \rightarrow I(m(\Lambda), \alpha(\Lambda)) \quad (3.9)$$

There is nothing different about this result, except that we have absorbed all of the divergent behavior into the physical parameters, so that I is no longer explicitly divergent, but merely dependent on divergent but physical quantities.

After all, we know that the electron is not infinitely massive or has infinite charge!" But what you are forgetting is that we have not yet specified our renormalization conditions yet. In fact, if we chose for our RC:

$$m(\Lambda) \rightarrow m_R \quad \alpha(\Lambda) \rightarrow \alpha_R \quad (3.10)$$

in the physical limit (the "R" stands for "renormalized"), then our final result is simply $I(m_R, \alpha_R)$ - a finite answer! m_R and α_R are now just the quantities we measure for the electron mass and charge respectively. We have literally "swept the infinities under the rug" to extract the UV-finite solution.

Before you label this as ridiculous, realize that QED has used renormalization all the time, and its results have been tested to as many as fourteen decimal places. That is the best-known confirmation of any theory of physics. Surely we must be doing something right!

As a final point, we wanted to mention that our final (finite) results could not depend on the regulator. However, you may be concerned about the process of absorbing the regulator into the physical quantities. For example, do you absorb any of the finite part of your regulated integral? Each regularization scheme gives you a different finite part, so how are you to know what to drop and what to keep? The answer is that you must explicitly state these details when you give your final answer. This final step is often called the subtraction scheme. So when you quote a final renormalized answer, you must state what subtraction scheme you used to renormalize the observable quantities.

3.3 The Schemes of Renormalization

All of the schemes of renormalization mark off the divergent and finite parts through fixed counterterms. The most simple renormalization scheme is the minimal subtraction (\overline{MS}) scheme, which is produced by the dimensional regularization naturally.

The parameters in counterterms are just the culmination terms in this scheme. In the dimensional regularization scheme, there is $\ln 4\pi - \gamma_E$, where γ_E is the Euler-constant in company with culmination terms. So $\ln 4\pi - \gamma_E$ belongs to the divergent parts of counterterms. This scheme is called corrected minimal subtraction (\overline{MS}) scheme. It is important to resolve the renormalization group equation because the upper two subtraction schemes are independent of mass. There are two other schemes must be introduced. They are momentum renormalization scheme and on-shell-mass renormalization scheme. In these two schemes, counterterms are fixed on the boundary conditions of propagators and vertice. In the momentum renormalization scheme, the boundary condition is confined by $p^2 = -\mu^2$. In the on-shell-mass renormalization scheme, the boundary condition is confined by $p^2 = m^2$. Here we know the on-shell-mass renormalization scheme is just the particular model of the momentum renormalization scheme when $\mu^2 = -m^2$. The on-shell-mass renormalization scheme is also called physical renormalization scheme.

3.4 Discussion

“Renormalization” is a word that has been given the evil eye by mathematicians, philosophers and popular science writers ever since it was first used to control infinities prevalent in quantum field theories. For a long time, many physicists have also looked down on it as a necessary although unattractive procedure. However, as quantum field theory becomes time tested again and again, it becomes harder to simply write off renormalization as a bad idea.

When Wilson, et al. published their derivation of the renormalization group, physics underwent a spectacular shift in philosophy. No longer was renormalization a necessary evil, but a requirement! It provided an entirely new way of interpreting ultraviolet divergences. The general philosophy of quantum field theorists is now that any given theory of physics has some energy scale where the theory breaks down. Renormalization not only allows you to perform calculations below that scale, but through the renormalization group equations, tells us where that scale is! This allows people to predict where to find new physics. For example, this is how people predicted the top quark mass, and currently motivates the search for supersymmetry, extra dimensions and other new theories.

Renormalization has not only helped us to explore the perturbative regime of quantum field theories, but has also given us great insight into the nature of how

physical theories must scale with energy. It has given us a way to deeply probe the nature of the theory itself. While mathematicians and philosophers continue to call it a problem, physicists have learned that it truly is our deeply misunderstood friend.

4 Feynman Diagrams and Feynman Rules of Process $\gamma\gamma \rightarrow e^+e^-$

4.1 Feynman Diagrams

4.1.1 Tree-level Diagrams of Process $\gamma\gamma \rightarrow e^+e^-$

The Feynman diagrams are drawn by Mathematica with FeynArts32^[38] package in this paper. The tree-level diagrams are shown in Fig.4.1.

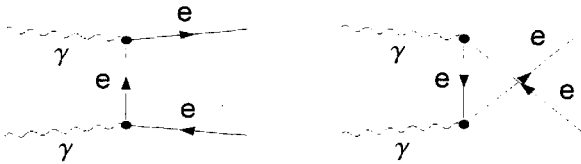
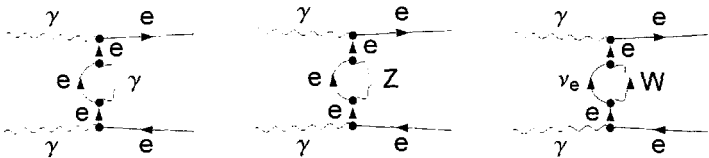


Fig.4.1 Lowest-order diagrams for process $\gamma\gamma \rightarrow e^+e^-$

4.1.2 One-loop Diagrams of Process $\gamma\gamma \rightarrow e^+e^-$

We will calculate the one-loop electroweak radiative corrections of process $\gamma\gamma \rightarrow e^+e^-$ in this paper, and draw its one-loop electroweak corrections diagrams in this chapter. The one-loop diagrams include self-energy (Fig.4.2), triangle (Fig.4.3), box diagrams (Fig.4.4) and their counterterms (Fig.4.5), where self-energy diagrams excluded the diagrams on external legs.



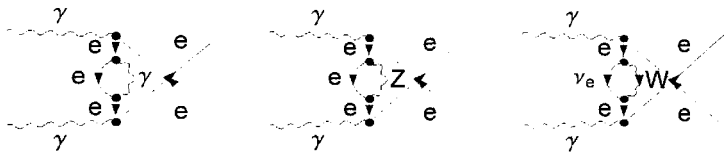
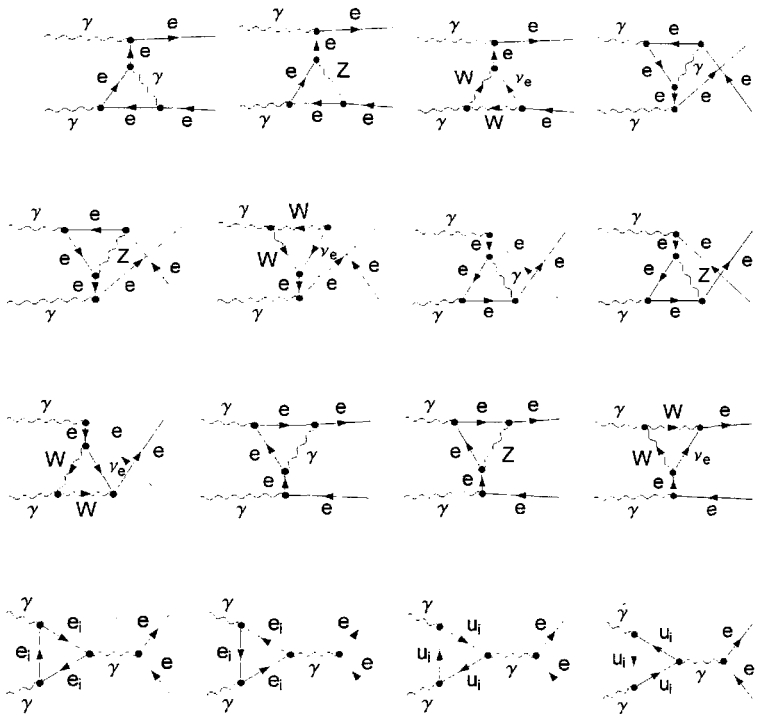
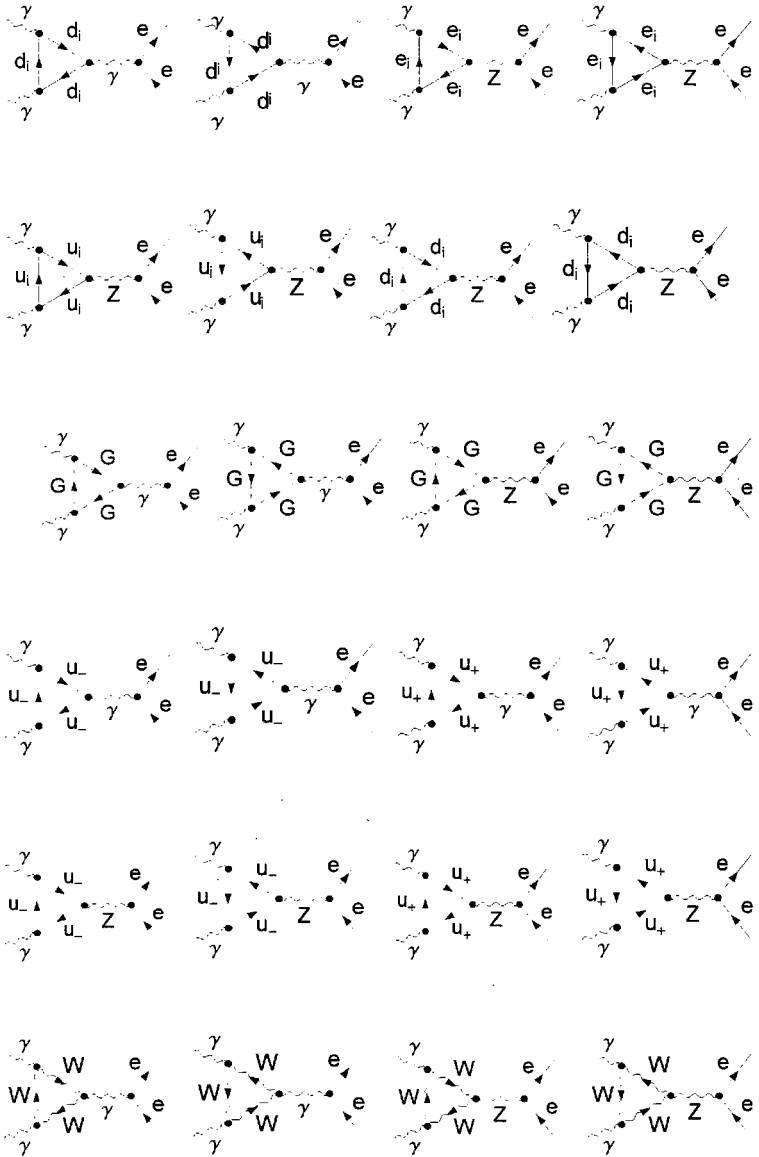
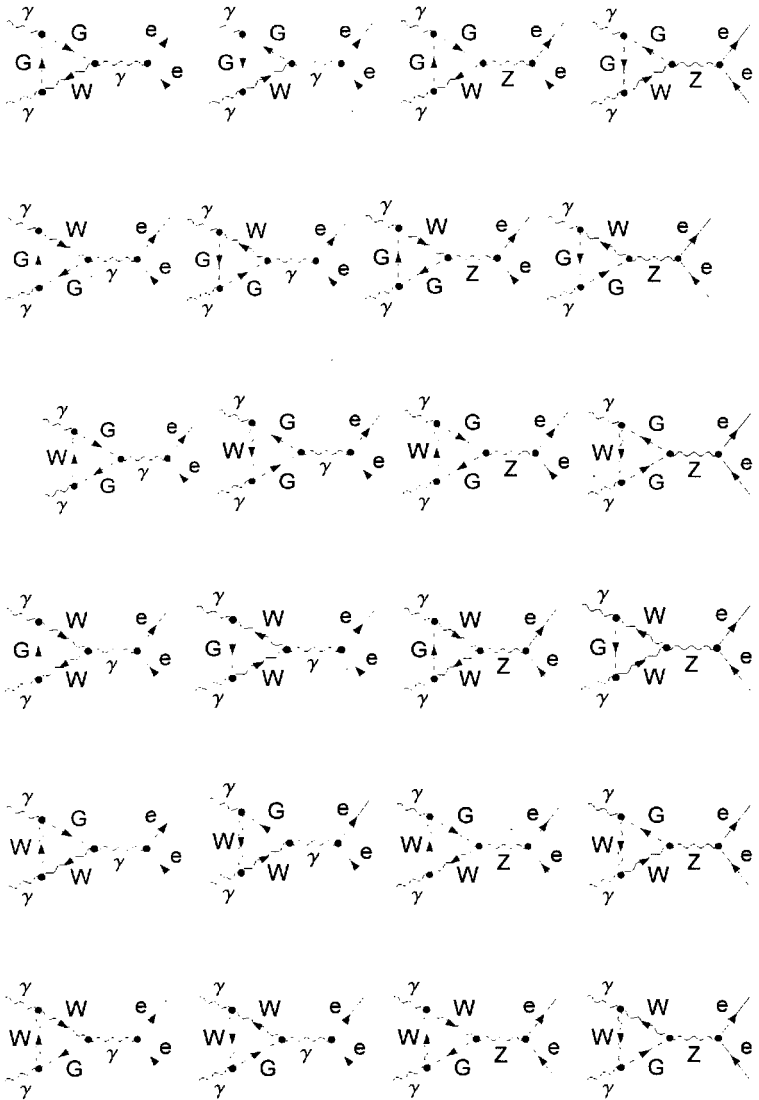


Fig.4.2 Self-energy diagrams







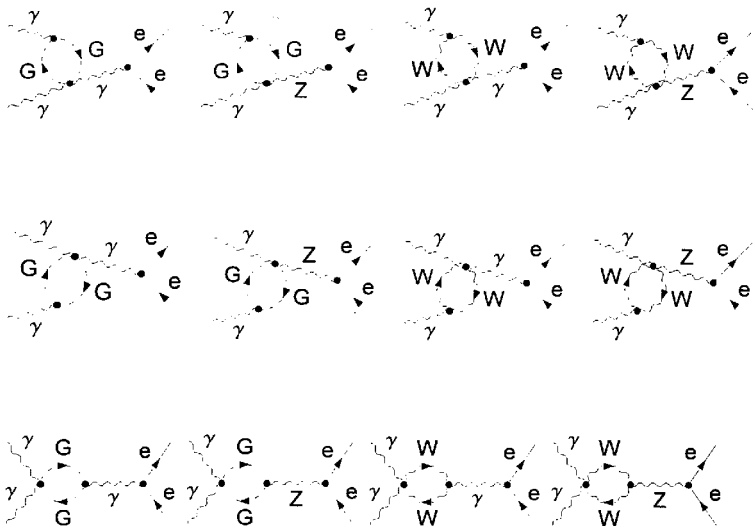
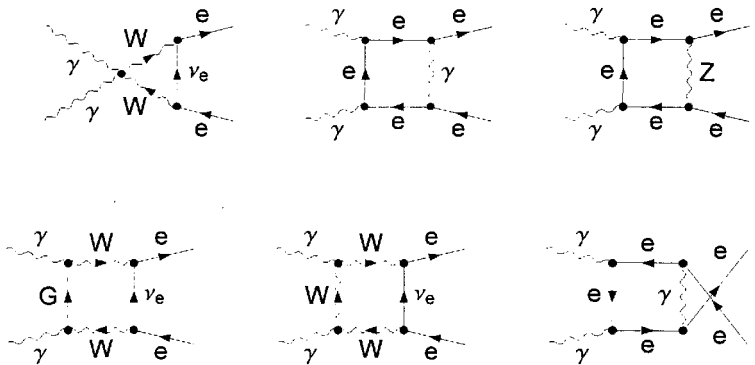


Fig.4.3 Triangle diagrams of process $\gamma\gamma \rightarrow e^+e^-$



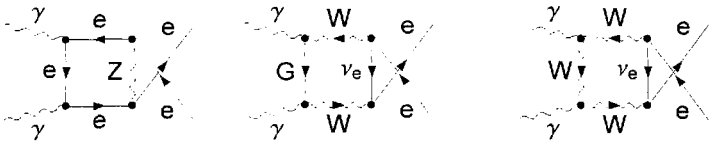


Fig.4.4 Box diagrams of process $\gamma\gamma \rightarrow e^+e^-$

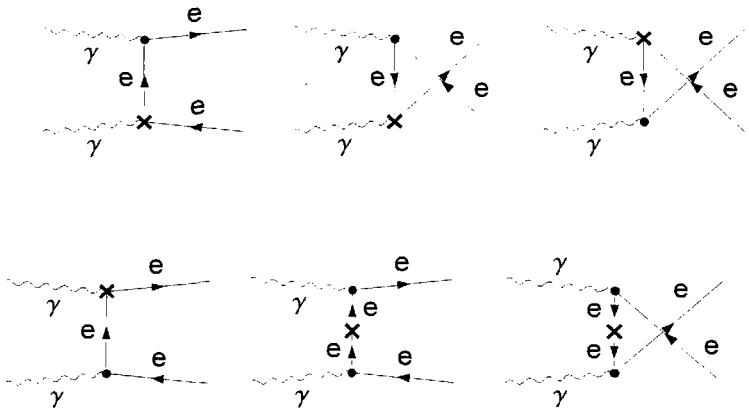
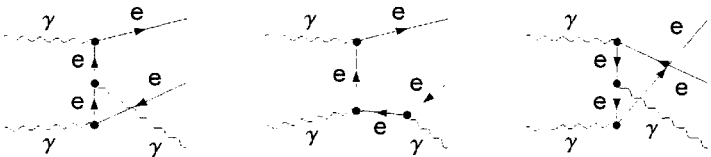


Fig.4.5 Counterterms of process $\gamma\gamma \rightarrow e^+e^-$



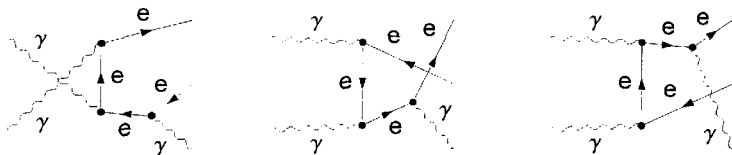
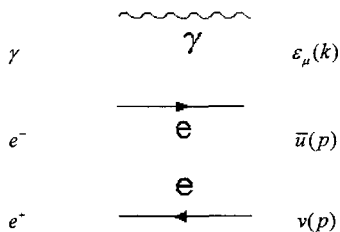


Fig.4.6 The real photon emissions of process $\gamma\gamma \rightarrow e^+e^-$

4.2 Feynman Rules

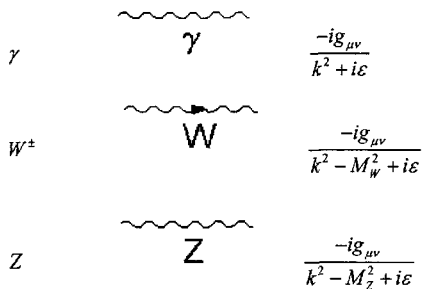
We adopt 't Hooft-Feynman gauge in this paper, i.e. $\xi=1$. We write down the Feynman rules of this process $\gamma\gamma \rightarrow e^+e^-$ here.

External legs:

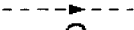

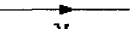



Propagators:

Gauge bosons



Higgs particles

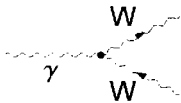
G^\pm		$\frac{i}{k^2 - M_W^2 + i\epsilon}$
Ghost particles		$\frac{i}{q^2 - M_W^2}$
Fermions		$\frac{ip}{p^2 + i\epsilon} \frac{1}{2}(1 - \gamma_5)$
$e_i(u_i, d_i)$		$\frac{i(p + m_e)}{p^2 - m_e^2 + i\epsilon}$

Vertex:

Three gauge fields coupling vertex



$$ig \cos \theta_w [g_{\eta\nu}(k-p)_\rho + g_{\nu\rho}(p-q)_\mu + g_{\rho\mu}(q-k)_\nu]$$

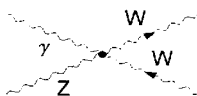


$$-ie[g_{\eta\nu}(k-p)_\rho + g_{\nu\rho}(p-q)_\mu + g_{\rho\mu}(q-k)_\nu]$$

Four gauge fields coupling vertex

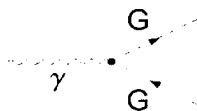


$$-ie^2(2g_{\mu\nu}g_{\lambda\rho} - g_{\mu\lambda}g_{\nu\rho} - g_{\mu\rho}g_{\nu\lambda})$$

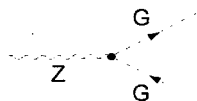


$$ieg \cos \theta_w (2g_{\mu\nu}g_{\lambda\rho} - g_{\mu\lambda}g_{\nu\rho} - g_{\mu\rho}g_{\nu\lambda})$$

One gauge field and two Higgs fields coupling vertice



$$ie(p-q)_\mu$$

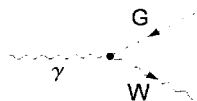


$$\frac{-ig \cos 2\theta_w}{2 \cos \theta_w} (p-q)_\mu$$

Two gauge fields and one Higgs field coupling vertice

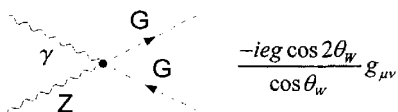


$$-igM_Z \sin^2 \theta_w g_{\mu\nu}$$

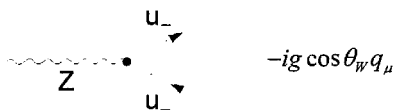
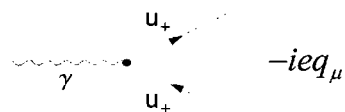
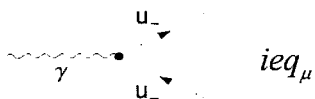


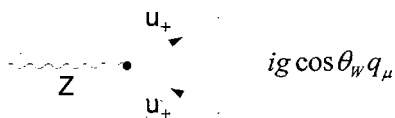
$$-ieM_W g_{\mu\nu}$$

Two gauge fields and two Higgs fields coupling vertice



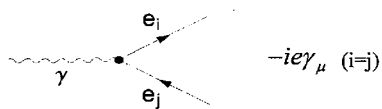
Ghost fields and gauge fields coupling vertice





$$ig \cos \theta_W q_\mu$$

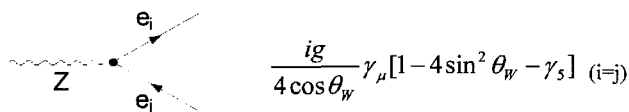
Lepton and gauge fields coupling vertice



$$-ie\gamma_\mu \quad (i=j)$$

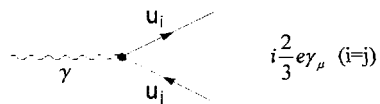


$$\frac{-ig}{2\sqrt{2}} \gamma_\mu (1 - \gamma_5)$$

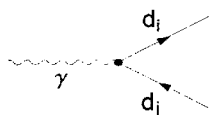


$$\frac{ig}{4 \cos \theta_W} \gamma_\mu [1 - 4 \sin^2 \theta_W - \gamma_5] \quad (i=j)$$

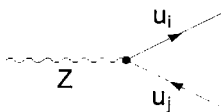
Quark and gauge fields coupling vertice



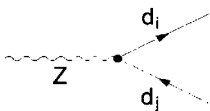
$$i\frac{2}{3}e\gamma_\mu \quad (i=j)$$



$$-i\frac{1}{3}e\gamma_\mu \quad (i=j)$$



$$-\frac{ig}{4\cos\theta_w}\gamma_\mu\left[1-\frac{8}{3}\sin^2\theta_w-\gamma_5\right] \quad (i=j)$$



$$\frac{ig}{4\cos\theta_w}\gamma_\mu\left[1-\frac{4}{3}\sin^2\theta_w-\gamma_5\right] \quad (i=j)$$

5 The Calculation of Cross-sections

5.1 The Tools We Adopted for Calculating Cross-sections

FormCalc is a Mathematica package for the calculation of tree-level and one-loop Feynman diagrams. It reads diagrams generated with FeynArts and returns the results in a way well suited for further numerical and analytical evaluation. FormCalc can in fact write out a complete Fortran subroutine to compute the squared matrix element for a given process.

The following simplifications are performed by FormCalc:

- Indices are contracted as far as possible,
- Fermion traces are evaluated,
- Open fermion chains are simplified using the Dirac equation,
- Colour structures are simplified using the $SU(N)$ algebra,
- The tensor reduction is done,
- Local terms (the remnants of divergent integrals) are added,
- The results are partially factored,
- Abbreviations are introduced.

The output is in general a linear combination of loop integrals with prefactors that contain model parameters, kinematic variables, and abbreviations introduced by FormCalc. Such abbreviations are introduced for spinor chains, scalar products of vectors, and epsilon tensors contracted with vectors.

FormCalc can treat ultraviolet divergences either with dimensional regularization or with constrained differential renormalization. At the one-loop level, the latter technique is equivalent to dimensional reduction. This means that FormCalc can process also supersymmetric diagrams.

The most common way to proceed with the analytical output is to convert it to a Fortran program. FormCalc has a sophisticated Fortran code generator built in which can produce a subroutine to calculate the squared matrix element fully automatically. This subroutine has to be linked with driver programs which supply the necessary input parameters. Included in the FormCalc package are driver programs for computing cross-sections of $1 \rightarrow 2$, $2 \rightarrow 2$, and $2 \rightarrow 3$ processes. It is written in a very modular way so that it is fairly easy to adapt parts of it for other purposes.

Internally, FormCalc performs most of the hard work (e.g. working out fermionic traces) in FORM, by Jos Vermaseren. The concept is rather straightforward: the symbolic expressions of the diagrams are prepared in an input file for FORM, then FORM is run, and finally the results are read back into Mathematica. The interfacing is completely shielded from the user and is handled internally by the FormCalc functions. The following diagram shows schematically how FormCalc interacts with FORM.

With the increasing accuracy of experimental data, one-loop calculations have in many cases come to be regarded as the lowest approximation acceptable to publish the results in a respected journal. FormCalc goes a big step towards automating these calculations.

FormCalc is a Mathematica package which calculates and simplifies tree-level and one-loop Feynman diagrams. It accepts diagrams generated with FeynArts [Ha00] and returns the results in a way well suited for further numerical (or analytical) evaluation.

A substantial part of the Mathematica code indeed acts as a driver that threads the FeynArts amplitudes through FORM in an appropriate way. The following diagram (Fig.5.1) shows schematically how FormCalc interacts with FORM.

FormCalc combines the speed of FORM with the powerful instruction set of Mathematica and the latter greatly facilitates further processing of the results. Owing to FORM's speed, FormCalc can process, for example, the 1000-odd one-loop diagrams of W - W scattering in the Standard Model in a few minutes on ordinary hardware.

One important aspect of FormCalc is that it automatically gathers spinor chains, scalar products of vectors, and antisymmetric tensors contracted with vectors, and introduces abbreviations for them. In calculations with non-scalar external particles where such objects are ubiquitous, code produced from the FormCalc output (say, in Fortran) can be significantly shorter and faster than without the abbreviations.

FormCalc can work in D and 4 dimensions. In D dimensions it uses standard dimensional regularization to treat ultraviolet divergences, in 4 dimensions it uses the method of constrained differential renormalization, which at one-loop level is equivalent to dimensional reduction.

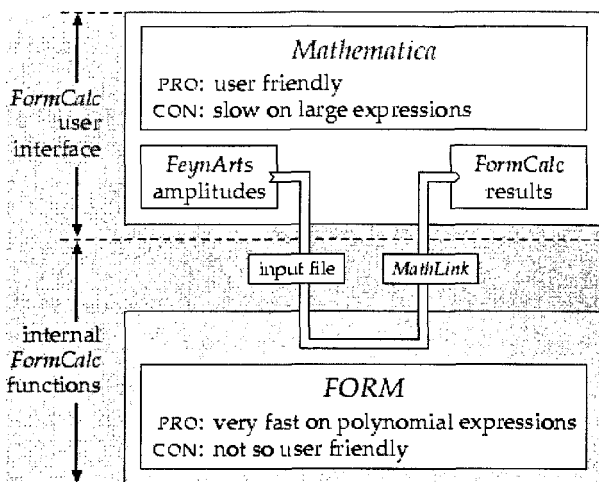


Fig. 5.1 How FormCalc interacts with FORM

A one-loop calculation generally includes three steps (Fig.5.2):

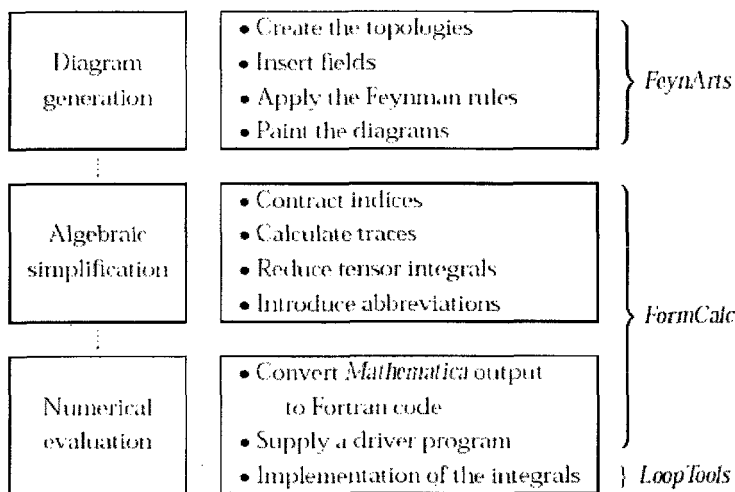


Fig.5.2 Three steps of a one-loop calculation

The automation of the calculation is fairly complete in FormCalc, i.e. FormCalc can eventually produce a complete Fortran program to calculate the squared matrix

element for a given process. The only thing the user has to supply is a driver program which calls the generated subroutines.

It is nevertheless important to realize that the Fortran code is generated only at the very end of the calculation (if at all), i.e. the calculation proceeds analytically as far as possible. At all intermediate stages, the results are Mathematica expressions which are considerably easier to modify than Fortran code.

In this paper, the editions of FeynArts、FormCalc、LoopTools we adopt are FeynArts32、FormCalc32 and LoopTools21. On the other hand, we adopt the Mathematica4 for Linux system to calculate the tree-level and one-loop corrected cross-sections. The gamma algebra and the one-loop integral functions are shown in Appendix B and C.

5.2 Notation and Conventions

We consider the reaction

$$\gamma(k_1, \lambda_1) + \gamma(k_2, \lambda_2) \rightarrow e^-(p_1, \sigma_1) + e^+(p_2, \sigma_2) \quad (5.1)$$

where k_1 and k_2 are the momentum of the incoming photons. The momentum of the outgoing electron and positron are p_1 and p_2 . $\lambda_{1,2} = \pm 1$ and $\sigma_{1,2} = \pm 1/2$ denote the helicities of the incoming photons and spin of outgoing electron(positron), respectively. If ignoring the masses of electron and positron, all the momentum follow the on-shell conditions: $k_1^2 = k_2^2 = 0$, $p_1^2 = p_2^2 = 0$. We define the Mandelstam variables

$$s = (k_1 + k_2)^2 = (p_1 + p_2)^2 \quad (5.2)$$

$$t = (k_1 - p_1)^2 = (k_2 - p_2)^2 \quad (5.3)$$

$$u = (k_1 - p_2)^2 = (k_2 - p_1)^2 \quad (5.4)$$

5.3 Lowest-order Cross-section

The two tree-level diagrams for $\gamma\gamma \rightarrow e^+e^-$ are shown in Fig.4.1. The corresponding amplitude is given by

$$M_{\text{tree}} = -ie^2 \bar{u}(p_2) \left\{ \gamma_\mu \frac{1}{(\not{k}_1 - \not{p}_1) - m_e} \gamma_\nu + \gamma_\nu \frac{1}{(\not{k}_1 - \not{p}_2) - m_e} \gamma_\mu \right\} v(p_1) \varepsilon(k_1) \varepsilon(k_2) \quad (5.5)$$

leading to the differential Born cross-section

$$\frac{d\sigma_{\text{tree}}}{d\Omega} = \sum_{\lambda_1, \lambda_2, \sigma_1, \sigma_2} \frac{\beta}{64\pi^2 s} |M_{\text{tree}}|^2 \quad (5.6)$$

where $\beta = \sqrt{1 - m_e^2/E^2}$ is the velocity of electron in center-mass system. The summation symbol denotes the spin summations of incoming and outgoing particles.

5.4 Radiative Corrections

In the loop diagram calculation we adopt the definitions of one-loop integral functions in reference^[41]. The one-loop electroweak radiative corrections diagrams and their counterterms of process $\gamma\gamma \rightarrow e^+e^-$ are shown in Fig.4.2-Fig.4.5. The corrected differential cross-section has the following form

$$\frac{d\sigma}{d\Omega} = \sum_{\lambda_1, \lambda_2, \sigma_1, \sigma_2} \frac{\beta}{64\pi^2 s} [|M_{\text{tree}}|^2 (1 + \delta_{\text{SB}}) + 2\{M_{\text{tree}}^* \delta M\}] = \frac{d\sigma_{\text{tree}}}{d\Omega} (1 + \delta) \quad (5.7)$$

δ_{SB} denotes the soft-photon bremsstrahlung factor, and δM the one-loop corrections to the transition amplitude. In this paper, δM including the contributions of self-energy, vertex, box and counterterm. The factor δ represents the complete relative correction and its definition is $\delta = (d\sigma - d\sigma_{\text{tree}})/d\sigma_{\text{tree}}$.

Integrated cross-section σ is defined the integral of differential cross-section in the range of detector

$$\sigma = \int_{\theta_{\text{min}}}^{\theta_{\text{max}}} d\cos\theta \int_0^{2\pi} d\phi \left(\frac{d\sigma}{d\Omega} \right) \quad (5.8)$$

From Fig.4.2-Fig.4.4, we acquired that there is UV divergence in loop diagrams, which can be regularized by extending the dimensions of spinor and spacetime manifolds to $D = 4 - 2\epsilon$ ^[42], and divide the divergence integrals into divergent part and finite part. In this paper, we adopt the complete on-mass-shell (COMS) renormalization scheme^{[43][44][45][46][47]} to fix all the renormalization constants. After introducing the counterterms, the divergent part and the counterterms counteract each other and we acquire the finite part. The UV divergence is removed, while the IR divergence still exists. So, we introduce the real photon emission (Fig4.6).

$$\gamma(k_1) + \gamma(k_2) \rightarrow e^-(p_1) + e^+(p_2) + \gamma(k) \quad (5.9)$$

By using the general phase-space-slicing algorithm^{[48][49][50]}, the contributions to photon emission process $\gamma\gamma \rightarrow e^+e^-\gamma$ are divided into a soft and a hard contribution,

$$\sigma_{\text{real}} = \sigma_{\text{soft}} + \sigma_{\text{hard}} \quad (5.10)$$

where the “soft” and “hard” refer to the energy of the radiated photon E_γ . The energy E_γ of the radiated photon in the center-mass frame is considered soft and hard if $E_\gamma \leq \Delta E$ and $E_\gamma > \Delta E$, respectively. Both σ_{soft} and σ_{hard} depend on the arbitrary soft cutoff $\Delta E/E_b$, where $E_b = \sqrt{s}/2$ is the photon beam energy in the center-mass frame, but the real cross section σ_{real} is cutoff independent. In this paper, we adopt $\Delta E = 0.1\sqrt{s}/2 = 0.05\sqrt{s}$. In other words, the resolve of monitor for photon energy is 10%, which is appropriate in LC.

In the soft-photon approximation for the bremsstrahlung process $\gamma\gamma \rightarrow e^+e^-(\gamma)$ only photons with energies below the cut-off energy $E < \Delta E$ are included. The IR divergence is regulated by an infinitesimal photon mass m_γ ; it cancels against the IR divergence of the virtual corrections. The soft-photon correction leads to the following correction factor to the lowest-order cross-section

$$\delta_{\text{SB}} = -\frac{\alpha}{\pi} \left\{ 2 \ln \frac{2\Delta E}{\lambda} + \frac{1}{\beta} \ln \left(\frac{1-\beta}{1+\beta} \right) + \frac{s-2m_e^2}{s\beta} \left[2 \ln \frac{2\Delta E}{\lambda} \ln \left(\frac{1-\beta}{1+\beta} \right) - 2 \text{Li}_2 \left(\frac{1-\beta}{1+\beta} \right) + \frac{1}{2} \ln^2 \left(\frac{1-\beta}{1+\beta} \right) + \frac{\pi^2}{3} - 2 \ln \left(\frac{1-\beta}{1+\beta} \right) \left(\frac{2\beta}{1+\beta} \right) \right] \right\} \quad (5.11)$$

which can be obtained from the general results of Ref.^[51]. The factor δ_{SB} does not depend on the polarizations of the produced fermions and of the incoming photons, and its dependence on virtual photon mass λ can be cancelled against the one in δ_{virtual} .

In this paper, considering the luminosity detector self has the energy distinguish lower limit for measuring photon, we can regard this lower limit as the divided value ΔE of soft and hard photons and regard the hard photon emission process can be distinguished from soft photon emission process $\gamma\gamma \rightarrow e^+e^-(\gamma)$ in experiment, so we need not consider the hard photon emission process and we assume $\Delta E = 0.05\sqrt{s}$. The total cross-section of the process $\gamma\gamma \rightarrow e^+e^-(\gamma)$ can be written in the form

$$\sigma_{\text{tot}} = \sigma_{\text{tree}} + \sigma_{\text{virtual}} + \sigma_{\text{soft}} = \sigma_{\text{tree}} (1 + \delta_{\text{tot}}) \quad (5.12)$$

where $\delta_{\text{tot}} = \delta_{\text{virtual}} + \delta_{\text{soft}}$.

6 Numerical Calculations and the Conclusions

6.1 Numerical Calculations

For the numerical calculations we use the following SM input parameters^[52]

$$\begin{array}{lll}
 m_e = 0.510998902\text{MeV} & m_\mu = 105.658357\text{MeV} & m_\tau = 1.77699\text{MeV} \\
 m_u = 66\text{MeV} & m_c = 1.2\text{GeV} & m_t = 174.3\text{GeV} \\
 m_d = 66\text{MeV} & m_s = 150\text{MeV} & m_b = 4.3\text{GeV} \\
 m_W = 80.423\text{GeV} & m_Z = 91.1876\text{GeV} & \alpha_{\text{ew}}^{-1}(0) = 137.03599976
 \end{array}$$

Table 6.1 The contributions of $\sigma_{\text{virtual+soft}}$ under different \sqrt{s} and UV regularization parameter C_{UV} , and the unit of cross-section is pb.

\sqrt{s} [GeV]	I ($C_{UV} = 10^{-7}$)	II ($C_{UV} = 10^{-1}$)
500	-0.79013460342046	-0.79013460342342
800	-0.34172120314175	-0.34172120314506
1000	-0.231317157038315	-0.231317157030110
1500	-0.115060099483280	-0.115060099483835

Table 6.2 The contributions of $\sigma_{\text{virtual+soft}}$ under different \sqrt{s} and IR regularization parameter m_γ , and the unit of cross-section is pb.

\sqrt{s} [GeV]	I ($m_\gamma = 10^{-10}$ GeV)	II ($m_\gamma = 10^{-1}$ GeV)
500	-0.79013460342046	-0.79013460343094
800	-0.34172120314175	-0.34172120315876
1000	-0.231317157038315	-0.231317157049061
1500	-0.115060099483280	-0.115060099487346

In Table6.1, we present some numerical results of the cross section $\sigma_{\text{virtual+soft}}$ for $\gamma\gamma \rightarrow e^+e^-(\gamma)$, where the soft cutoff ΔE and the IR regularization parameter m_γ are set to be $\Delta E = 0.05\sqrt{s}$ and $m_\gamma = 10^{-10}$ GeV, respectively. The second and third columns are corresponding to the cases of $C_{UV} = 10^{-7}$ and $C_{UV} = 10^{-1}$, respectively. We

reserve the output numbers with 15 digits. By comparing the two columns of output numbers, we find that the results are stable over 11 digits when varying the UV regularization parameter C_{UV} from 10^{-7} to 10^{-1} . Therefore, we draw a conclusion that the cross section $\sigma_{\text{virtual+soft}}$ is independent of UV regularization parameter C_{UV} within the statistical error.

In Table 6.2, we also present some numerical results of the cross section $\sigma_{\text{virtual+soft}}$ for $\gamma\gamma \rightarrow e^+e^-(\gamma)$, where the soft cutoff ΔE and the UV regularization parameter C_{UV} are set to be $\Delta E = 0.05\sqrt{s}$ and $C_{UV} = 10^{-7}$, respectively. The second and third columns are corresponding to the cases of $m_\gamma = 10^{-10}$ GeV and $m_\gamma = 10^{-1}$ GeV, respectively. We reserve the output numbers with 15 digits also. By comparing the two columns of output numbers, we find that the results are stable over 10 digits when varying the IR regularization parameter m_γ from 10^{-10} to 10^{-1} GeV. Therefore, we draw a conclusion that the cross section $\sigma_{\text{virtual+soft}}$ is independent of IR regularization parameter m_γ within the statistical error.

We have calculated the one-loop virtual and soft-photon radiative corrections to $\gamma\gamma \rightarrow e^+e^-$ in the electroweak Standard Model. The tree-level and one-loop integrated cross sections are shown in Fig. 6.1. The upper solid line represent tree-level integrated cross section and the lower dash line is the one-loop electroweak corrected integrated cross section. The unit of integrated cross sections is pb, where $1\text{pb} = 10^{-12} \times 10^{-24} \text{cm}^2$ and the ranges of integral are $50\text{mrad} \leq \theta \leq 150\text{mrad}$ and the relevant $(\pi - 0.15)\text{rad} \leq \theta \leq (\pi - 0.05)\text{rad}$. On the other hand, the c.m. energy \sqrt{s} increases from 300 GeV to 1200 GeV. Because of the small mass of two outgoing electron and positron, the threshold value of the process of electron pair production through two photons collision is very small, about 0.01 GeV. So we can't find the peak value of integrated cross sections increasing with c.m. energy \sqrt{s} , but two gradually decreasing lines. From the Fig. 6.1, we also find that the one-loop electroweak correction to tree-level integrated cross-section is very large for the process

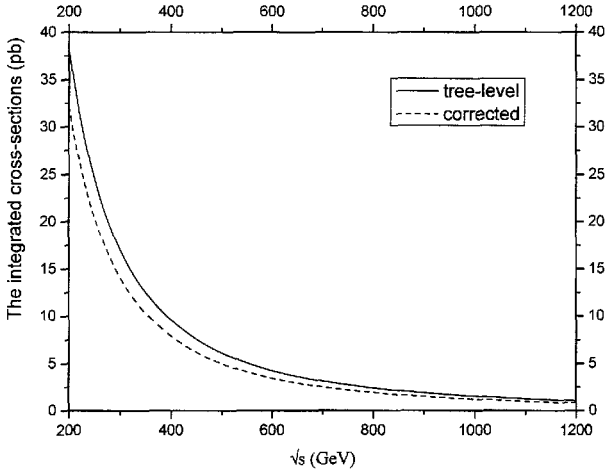


Fig.6.1 the curve relationship between the tree-level and one-loop integrated cross-sections and the energy of center-mass.

$\gamma\gamma \rightarrow e^+e^-$. The relative correction reaches at -18.5% for the c.m. energy $\sqrt{s}=500\text{GeV}$ and at -21.1% for the c.m. energy $\sqrt{s}=1000\text{GeV}$.

We draw the differential cross-sections with different angular cut, which the angular cut $50\text{mrad} \leq \theta \leq 150\text{mrad}$ is shown in Fig.6.2 and the angular cut $(\pi - 0.15)\text{rad} \leq \theta \leq (\pi - 0.05)\text{rad}$ is shown in Fig.6.3. The upper two lines in Fig.6.2 and Fig.6.3 are the cross-sections at $\sqrt{s}=500\text{GeV}$ and the middle two lines are the cross-sections at $\sqrt{s}=800\text{GeV}$ and the lowest two lines are the cross-sections at $\sqrt{s}=1200\text{GeV}$. The solid lines represent the tree-level differential cross-sections and the dash lines represent the one-loop corrected differential cross-sections in the upper two figures. From Fig.6.2 and Fig.6.3, we can draw a conclusion that the outgoing particles concentrate on a very little angle. The range of the luminosity detector at GLC is $50\text{mrad} \leq \theta \leq 150\text{mrad}$ and $(\pi - 0.15)\text{rad} \leq \theta \leq (\pi - 0.05)\text{rad}$, which can

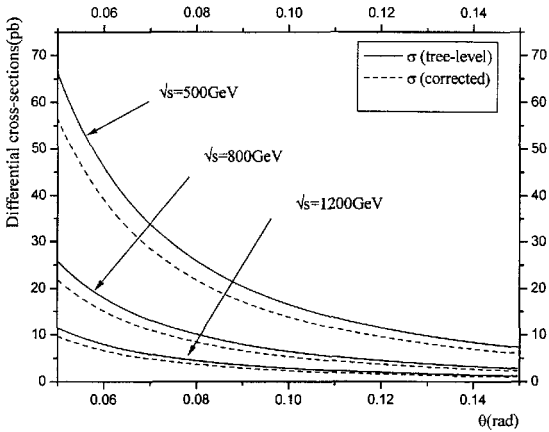


Fig.6.2 the tree-level and the one-loop corrected differential cross-sections at different c.m. energy with an angular cut $50\text{mrad} \leq \theta \leq 150\text{mrad}$.

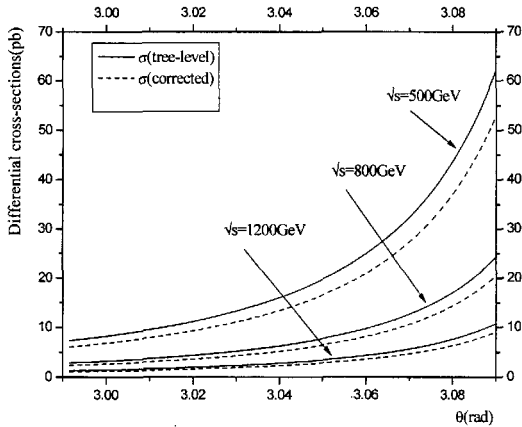


Fig.6.3 the tree-level and the one-loop corrected differential cross-sections at different c.m. energy with an angular cut $(\pi - 0.15)\text{rad} \leq \theta \leq (\pi - 0.05)\text{rad}$.

seize a majority of outgoing particles. We also find that the one-loop corrections are relatively great.

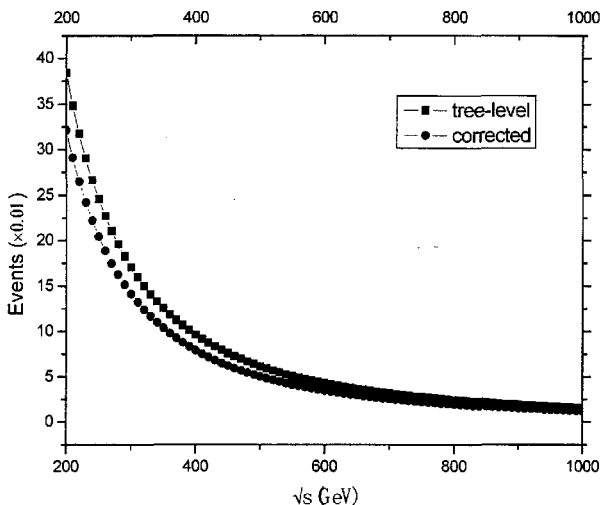


Fig.6.4 The events in different center-mass energy

We also draw the relation curve between the numbers of events and center-mass energy, which was shown in Fig.6.4. The numbers of events is luminosity monitor accept events per second and the definition of the numbers of events is

$$N = \sigma \times L \quad (6.1)$$

where N is the numbers of events, σ is the cross-section and L is the luminosity of monitor. The luminosity we choose in this paper is $10^{34} \text{ cm}^{-2} \text{ s}^{-1}$ at GLC. We can see from the Fig.6.4 that the events are in proportion with cross-sections. We draw the curve between the numbers of events and angular distributions in Fig.6.5 and Fig.6.6 at the end of this paper.

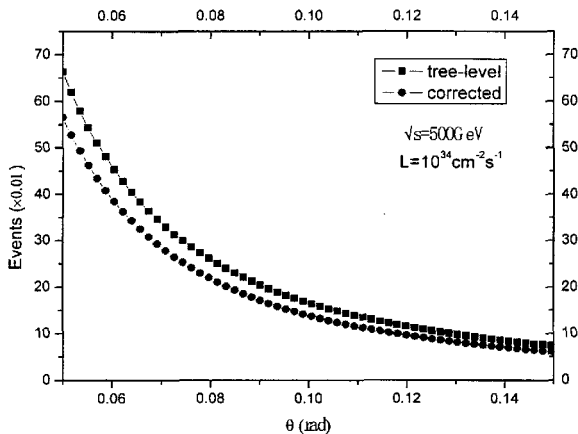


Fig.6.5 the events in different angular distributions ($50\text{mrad} \leq \theta \leq 150\text{mrad}$)

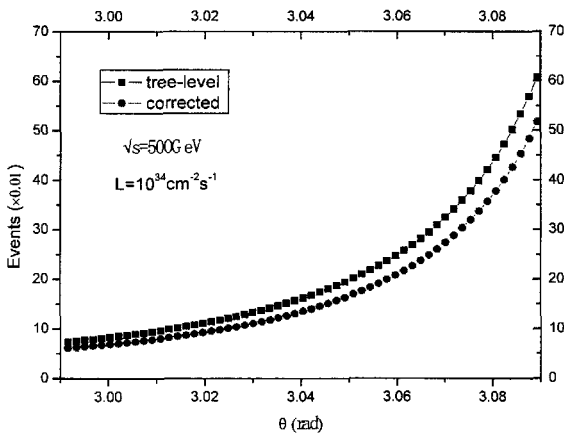


Fig.6.6 Same to Fig.6.5, except the angular distribution is $(\pi - 0.15)\text{rad} \leq \theta \leq (\pi - 0.05)\text{rad}$

6.2 Summary and Prospect

In this paper we calculate the electro weak corrections to $\gamma\gamma \rightarrow e^+e^-$ at GLC in the SM, and obtain the cross-sections are independent of UV divergent parameter and IR divergent parameter. We analyze the dependence of the tree-level cross-section and the corrected cross-section including virtual corrections and soft photon correction on the center-mass energy. We find the corrections are very large at some energy, so the corrections should be considered in calculations and the cross-sections are relative large, the process $\gamma\gamma \rightarrow e^+e^-$ is a very prospective process in future colliders. The angular distributions of the luminosity monitor at GLC are $50\text{mrad} \leq \theta \leq 150\text{mrad}$ and $(\pi - 0.15)\text{rad} \leq \theta \leq (\pi - 0.05)\text{rad}$. We also adopt these ranges to calculate the integral cross-sections and differential cross-sections. The numbers of events at different center-mass energy and angular ranges are acquired in the end of the numerical calculations. The luminosity of monitor at GLC is $10^{34}\text{cm}^{-2}\text{s}^{-1}$.

The Standard Model answers many of the questions about the structure and stability of matter with its six types of quarks, six types of leptons, and four forces. But the Standard Model is not complete; there are still many unanswered questions:

Why do we observe matter and almost no antimatter if we believe there is a symmetry between the two in the universe?

What is this "dark matter" that we can't see that has visible gravitational effects in the cosmos?

Why can't the Standard Model predict a particle's mass?

Are quarks and leptons actually fundamental, or made up of even more fundamental particles?

Why are there exactly three generations of quarks and leptons?

How does gravity fit into all of this?

Today, one of the major goals of particle physics is to unify the various fundamental forces in a Grand Unified Theory which could offer a more elegant understanding of the organization of the universe. Such a simplification of the Standard Model might well help to answer our questions and point toward future areas of study.

Physicists hope that a Grand Unified Theory will unify the strong, weak, and electromagnetic interactions. There have been several proposed Unified Theories, but we need data to pick which, if any, of these theories describes nature.

If a Grand Unification of all the interactions is possible, then all the interactions we

observe are all different aspects of the same, unified interaction. However, how can this be the case if strong and weak and electromagnetic interactions are so different in strength and effect? Strangely enough, current data and theory suggests that these varied forces merge into one force when the particles being affected are at a high enough energy [Fig.6.7].

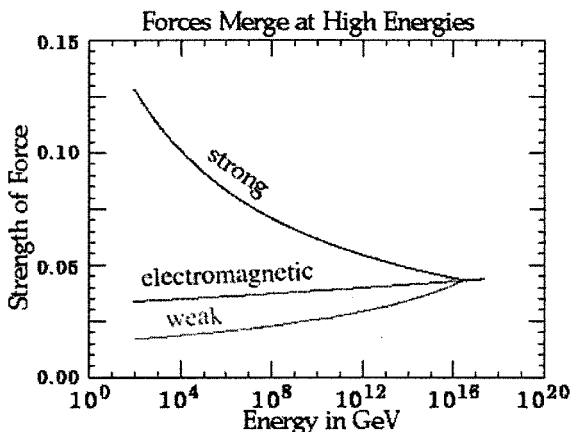


Fig.6.7 Varied forces merge into one force when the particles being affected are at a high enough energy.

Current work on GUT suggests the existence of another force-carrier particle that causes the proton to decay. Such decays are extremely rare; a proton's lifetime is more than 10^{32} years.

致 谢

本论文是在我的导师方祯云教授和胡炳全副教授的悉心指导下完成的。在此，我要向方老师和胡老师表示最衷心的感谢和最深厚的敬意！三年来，方老师在各个方面都给予了我极大的帮助。在学习上，方老师给我指明了学习的方法，让我受益匪浅，使我少走了不少弯路，渐渐地具有了一定的理论物理头脑。方老师也为我外出学习提供了许多便利的条件，使我了解到了许多理论物理方面的新动向、新知识，并且学到了许多解决问题的方法，为我将来的继续学习深造提供了条件。方老师严谨的科学作风、渊博的知识以及对工作的一丝不苟的态度，对我都是非常大的震撼，将让我终生受益。胡老师热情的态度、渊博的知识也让我收益颇多。尤其是在胡老师的指导下，让我学到了理论物理研究的基本方法，这对我将来的学习、工作都会有极大的帮助。我还要特别地感谢中国科学技术大学近代物理系的马文淦教授！感谢马老师给我提供了优越的学习、生活条件，让我可以顺利完成此篇论文。我还要感谢马老师对此论文给予的指导。马老师为人和蔼，知识渊博，事必躬亲的态度都给我留下了深刻的印象。

我还要感谢三年来指导我完成理论物理基础课程学习的张忠灿教授、李芳昱教授！是你们让我拥有了坚实的理论物理基础，对我论文的完成提供了保障。

我的论文的完成也离不开理论所各位同学的帮助！感谢陈刚、罗光、吴张晗、张义、史琳娜等。我与他们在理论所共同度过了三年愉快的学习生活。我还要感谢李志峰师兄的帮助，感谢他为我解答疑问及查阅资料。我也要感谢理论所里所有的师弟师妹对我完成论文期间给予的支持。

我要感谢我的父母的养育之恩以及父母、哥嫂给予我在经济和精神上的支持。我还要感谢我的男友邓剑勋。感谢他对我生活的照顾，让我能够安心完成论文。

在此，向帮助、指导我论文完成的所有老师、同学及家人表示由衷的谢意！

衷心地感谢在百忙之中评阅论文和参加答辩的各位专家、教授！

曾代敏

二〇〇四年五月

Reference

- [1] S.Weinberg, Phys.Rev.Lett.**19** (1967) 1264.
- [2] A.Salam, Proceedings of 8th Nobel Symposium (Atockholm), edited by N.Svartholm (Almqvist and Wiksell, Stockholm, 1968)p.367.
- [3] S.Glashow, Nucl.Phys.**22** (1961) 579.
- [4] F. Abe et al., CDF collaboration, FERMILAB-PUB-95/022-E, hep-ex/9503002.
- [5] S. Abachi et al., DØ collaboration, FERMILAB-PUB-95/028-E, hep-ex/9503003.
- [6] I.F. Ginzburg, G.L. Kotkin, V.G. Serbo and V.I. Telnov, Nucl. Instr. Meth. **205**(1983) 47.
- [7] I.F. Ginzburg, G.L. Kotkin, S.L. Panfil, V.G. Serbo and V.I. Telnov, Nucl.Instr.Meth. **219** (1984) 5.
- [8] V.I. Telnov, Nucl. Instr. Meth. **A294** (1990) 72.
- [9] F. Abe et al., CDF collaboration, FERMILAB-PUB-95/036-E, hep-ex/9503009.
- [10] I.F. Ginzburg, G.L. Kotkin, V.G. Serbo and V.I. Telnov, Nucl. Instr. Meth. **205** (1983) 47; I.F. Ginzburg, G.L. Kotkin, S.L. Panfil, V.G. Serbo and V.I. Telnov, Nucl. Instr.Meth. **219** (1984) 5; Telnov, Nucl. Instr. Meth. **A294** (1990) 72;
- [11] Ginzburg, G. Kotkin, V. Serbo and V. Telnov, Pizma ZhETF, **34** (1981) 514; JETP Lett. **34**(1982) 491. Preprint INP 81-50, 1981, Novosibirsk.
- [12] Ginzburg, G. Kotkin, V. Serbo and V. Telnov, Nucl. Instr. & Meth. **205** (1983) 47, Preprint INP 81-102, 1991, Novosibirsk.
- [13] Ginzburg, G. Kotkin, S. Panfil, V. Serbo and V. Telnov, Nucl. Instr. & Meth. **219** (1984) 5.
- [14] I.F. Ginzburg, G.L. Kotkin, V.G. Serbo and V.I. Telnov, Nucl. Instr. Meth. **205** (1983) 47; I.F. Ginzburg, G.L. Kotkin, S.L. Panfil, V.G. Serbo and V.I. Telnov, Nucl. Instr. Meth. **219** (1984) 5.
- [15] E. Accomando et al. [ECFA/DESY LC Physics Working Group Collaboration], Phys.Rept. **299** (1998) 1 [hep-ph/9705442].
- [16] J. A. Aguilar-Saavedra et al., TESLA Technical Design Report Part III: Physics at an e+e- Linear Collider [hep-ph/0106315].
- [17] K. Abe et al. [ACFA Linear Collider Working Group Collaboration], ACFA Linear Collider Working Group report, [hep-ph/0109166].
- [18] T. Abe et al. [American Linear Collider Working Group Collaboration], in Proc. of the APS/DPF/DPB Summer Study on the Future of Particle Physics (Snowmass 2001) ed. R. Davidson and C. Quigg, SLAC-R-570, Resource book for Snowmass 2001 [hep-ex/0106055,

- hep-ex/0106056, hep-ex/0106057, hep-ex/0106058].
- [19] R. Brinkmann et al., Nucl. Instr. Meth. **A406** (1998) 13.
- [20] N. Akasaka et al., "JLC design study", KEK-REPORT-97-1.
- [21] J. K"ublbeck, M. B"ohm and A. Denner, Comp. Phys. Commun. **60** (1990) 165; H. Eck and J. K"ublbeck, Guide to FeynArts 1.0, University of W"urzburg, 1992.
- [22] S. Brodsky and P.M. Zerwas, Nucl. Instr. Meth. **A355** (1995) 19.
- [23] M. Chanowitz, Nucl. Instr. Meth. **A355** (1995) 42.
- [24] I. Ginzburg, Nucl. Instr. Meth. **A355** (1995) 63.
- [25] S.L.Glashow, Nucl.Phys.**22** (1961),579.
- [26] S.Weinberg, Phys.Rev.Lett.**19** (1967),1264.
- [27] A.Salam in Elementary Particle Physics (Nobel Symp. N.8), Ed. N.Svartholm, Almquist and Wiksells, Stockholm (1968), p.367.
- [28] For an introduction to the Symmetry Breaking Sector of the Electroweak Theory see, 'Introduction to the Symmetry Breaking Sector', M. Herrero, Proceedings of the XXIII International Meeting on Fundamental Physics, Comillas, Santander, Spain, May 1995, Eds. T.Rodrigo and A.Ruiz. World Sci.Pub.Co (1996), p.87.
- [29] Y.Nambu, Phys.Rev.Lett.4 (1960), 380.
- [30] J.Goldstone, Nuovo Cimento **19** (1961),154.
- [31] Bernstein.J.Spontaneous Symmetry Breaking, gauge theory, the higgs mechanism and all that.Rev.Mod.Phys.46, 7 (1974).
- [32] P.W.Higgs, Phys.Lett.**12** (1964), 132.
- [33] F.Englert and R.Brout, Phys.Rev.Lett.(1964),321.
- [34] G.S.Guralnik, C.R.Hagen and T.W.B.Kibble, Phys.Rev.Lett.**13** (1964) 585;
- [35] P.W.Higgs, Phys.Rev.**145** (1966), 1156.
- [36] T.W.B.Kibble, Phys.Rev.**155** (1967),1554.
- [37] UA1 Collaboration, G.Arnison et al., Phys.Lett.**B122** (1983) 103; UA2 Collaboration, M.Banner et al., Phys.Lett.**B122** (1983)476.
- [38] J. K"ublbeck, M. B"ohm and A. Denner, Comp. Phys. Commun. **60** (1990) 165; H. Eck and J. K"ublbeck, Guide to FeynArts 1.0, University of W"urzburg, 1992.
- [39] Y.Nambu, Phys.Rev.Lett.4 (1960), 380.
- [40] J.Goldstone, Nuovo Cimento **19** (1961), 154.
- [41] Bernd A. Kniehl, Phys. Rep. **240** (1994) 211.
- [42] G. 't Hooft and M. Veltman, Nucl. Phys. **B44**, 189 (1972).
- [43] Denner, Fortschr. Phys. **41**, 307 (1993).

- [44] D.A. Ross and J.C. Taylor, Nucl. Phys. **B51**, (1979)25.
- [45] Goto and T. Kon, Europhys. Lett. **13** (1990)211; 14 (1991)75.
- [46] F. Cuypart, G.J. Oldenborgh and R. Ruckl, Nucl. Phys.**B409**, (1993)144.
- [47] M. Hoike, T. Nonaka and T. Kon, Phys. Lett. **B357** (1995)232.
- [48] W. T. Giele and E. W. Glover, Phys. Rev. **D46**, 1980 (1992).
- [49] W. T. Giele, E. W. Glover and D. A. Kosower, Nucl. Phys. **B403**, 633 (1993);.
- [50] S. Keller and E. Laenen, Phys. Rev. **D59**, 114004 (1999).
- [51] Denner, Fortschr. Phys. **41**(1993) 307.
- [52] K. Hagiwara, et al., Phys. Rev. **D66**, 010001 (2002).

Appendix A

作者在攻读硕士学位期间发表的论文目录

- [1] 曾代敏, 方祯云, 胡炳全, 李志峰, 标准模型下双光子碰撞产生电子对的弱电辐射修正, 重庆大学学报(自然科学版)(已接收)
- [2] 张忠灿, 罗光, 方祯云, 曾代敏, 张宇, 介子圈图传播子重整化有限量的有效计算方法 I, 重庆大学学报(自然科学版)(已接收)
- [3] 张忠灿, 曾代敏, 方祯云, 罗光, 张宇, 介子圈图传播子重整化有限量的有效计算方法 II, 重庆大学学报(自然科学版)(待发表)
- [4] 罗光, 曾代敏, 张宇, 核子与核子在链圈图下的散射截面, 重庆大学学报(自然科学版)(待发表)

Appendix B

SCALAR ONE-LOOP INTEGRALS

The one-point function

The one-point function is given by

$$A(m^2) = \int d^n q \frac{1}{q^2 + m^2} = m^2(-\Delta - 1 + \ln m^2) \quad (\text{B.1})$$

where $\Delta = -\frac{2}{n-4} + \gamma - \ln \pi$ and $\gamma = \text{Eulers constant}$.

The two-point function

The two-point integrals occurring are

$$B_0; B_\mu; B_{\mu\nu}(p, m_1, m_2) = \frac{1}{i\pi^2} \int d^n q \frac{1; q_\mu; q_\mu q_\nu}{(q^2 + m_1^2)((q+p)^2 + m_2^2)} \quad (\text{B.2})$$

The function B_μ must be proportional to p_μ :

$$B_\mu(p, m_1, m_2) = p_\mu B_1(p, m_1, m_2) \quad (\text{B.3})$$

This defines the functions B_1 . Similarly:

$$B_{\mu\nu} = p_\mu p_\nu B_{21} + \delta_{\mu\nu} B_{22} \quad (\text{B.4})$$

The three-point function

The relevant integrals are:

$$\begin{aligned} C_0; C_\mu; C_{\mu\nu}; C_{\mu\nu\alpha}(p_1, p_2, m_1, m_2, m_3) \\ = \frac{1}{i\pi^2} \int d^n q \frac{1; q_\mu; q_\mu q_\nu; q_\mu q_\nu q_\alpha}{(q^2 + m_1^2)((q+p_1)^2 + m_2^2)((q+p_1+p_2)^2 + m_3^2)} \end{aligned} \quad (\text{B.5})$$

We write p and k instead of p_1 and p_2 . Here:

$$C_\mu = p_\mu C_{11} + k_\mu C_{12} \quad (\text{B.6})$$

$$C_{\mu\nu} = p_\mu p_\nu C_{21} + k_\mu k_\nu C_{22} + \{pk\}_{\mu\nu} C_{23} + \delta_{\mu\nu} C_{24} \quad (\text{B.7})$$

$$C_{\mu\nu\alpha} = p_\mu p_\nu p_\alpha C_{31} + k_\mu k_\nu k_\alpha C_{32} + \{kpp\}_{\mu\nu\alpha} C_{33} + \{pkk\}_{\mu\nu\alpha} C_{34} + \{p\delta\}_{\mu\nu\alpha} C_{35} + \{k\delta\}_{\mu\nu\alpha} C_{36} \quad (\text{B.8})$$

$$\{pk\}_{\mu\nu} = p_\mu k_\nu + k_\mu p_\nu \quad (\text{B.9})$$

$$\{kpp\}_{\mu\nu\alpha} = k_\mu p_\nu p_\alpha + p_\mu k_\nu p_\alpha + p_\mu p_\nu k_\alpha \quad (\text{B.10})$$

$$\{p\delta\}_{\mu\nu\alpha} = p_\mu \delta_{\nu\alpha} + p_\nu \delta_{\mu\alpha} + p_\alpha \delta_{\mu\nu} \quad (\text{B.11})$$

The four-point function

The relevant integrals are:

$$D_0; D_\mu; D_{\mu\nu}; D_{\mu\nu\alpha}; D_{\mu\nu\alpha\beta} = \frac{1}{i\pi^2} \times \int d^n q \frac{1; q_\mu; q_\mu q_\nu; q_\mu q_\nu q_\alpha; q_\mu q_\nu q_\alpha q_\beta}{(q^2 + m_1^2)((q + p_2)^2 + m_2^2)((q + p_1 + p_2)^2 + m_3^2)((q + p_1 + p_2 + p_3)^2 + m_4^2)} \quad (\text{B.12})$$

We use p, k and l instead of p_1, p_2 and p_3 , so we have:

$$D_\mu = p_\mu D_{11} + k_\mu D_{12} + l_\mu D_{13} \quad (\text{B.13})$$

$$D_{\mu\nu} = p_\mu p_\nu D_{21} + k_\mu k_\nu D_{22} + l_\mu l_\nu D_{23} + \{pk\}_{\mu\nu} D_{24} + \{pl\}_{\mu\nu} D_{25} + \{kl\}_{\mu\nu} D_{26} + \delta_{\mu\nu} D_{27} \quad (\text{B.14})$$

In the equations below we drop the indices μ, ν etc.

$$D_{\mu\nu\alpha} = pppD_{31} + kkkD_{32} + lllD_{33} + \{kpp\}D_{34} + \{lpp\}D_{35} + \{pkk\}D_{36} + \{pll\}D_{37} + \{lkk\}D_{38} + \{kll\}D_{39} + \{pkl\}D_{310} + \{p\delta\}D_{311} + \{k\delta\}D_{312} + \{l\delta\}D_{313} \quad (\text{B.15})$$

$$D_{\mu\nu\alpha\beta} = ppppD_{41} + kkkkD_{42} + llllD_{43} + \{pppk\}D_{44} + \{pppl\}D_{45} + \{kkkp\}D_{46} + \{kkkl\}D_{47} + \{lllp\}D_{48} + \{lllk\}D_{49} + \{ppkk\}D_{410} + \{ppll\}D_{411} + \{kkll\}D_{412} + \{ppkl\}D_{413} + \{kklp\}D_{414} + \{llpk\}D_{415} + \{pp\delta\}D_{416} + \{kk\delta\}D_{417} + \{ll\delta\}D_{418} + \{pk\delta\}D_{419} = \{pl\delta\}D_{420} + \{kl\delta\}D_{421} + \{\delta\delta\}D_{422} \quad (\text{B.16})$$

Appendix C

γ algebra

γ matrices

$$\gamma_5 = i\gamma^0\gamma^1\gamma^2\gamma^3 \quad (C.1)$$

$$\gamma^0 = \begin{pmatrix} 1 & 0 \\ 0 & -1 \end{pmatrix}, \quad \vec{\gamma} = \begin{pmatrix} 0 & \vec{\sigma} \\ -\vec{\sigma} & 0 \end{pmatrix} \quad (C.2)$$

where $\vec{\sigma}$ is Pauli matrix
fundamental anticommutator

$$\{\gamma^\mu, \gamma^\nu\} = 2g^{\mu\nu} \quad (C.3)$$

γ_5 identities

$$\gamma_5 = \begin{pmatrix} 0 & 1 \\ 1 & 0 \end{pmatrix}, \quad \{\gamma_5, \gamma^\mu\} = 0 \quad (C.4)$$

Trace theorems

$$Tr 1 = 4 \quad (C.5)$$

$$Tr \gamma_5 = 0 \quad (C.6)$$

$$Tr(\text{odd number of } \gamma\text{'s}) = 0 \quad (C.7)$$

$$Tr(a\bar{b}) = 4a \cdot b \quad (C.8)$$

$$Tr(a\bar{b}c\bar{d}) = 4[(a \cdot b)(c \cdot d) + (a \cdot d)(b \cdot c) - (a \cdot c)(b \cdot d)] \quad (C.9)$$

$$Tr[\gamma_5 a\bar{b}] = 0 \quad (C.10)$$

$$Tr[\gamma_5 a\bar{b}c\bar{d}] = 0 \quad (C.11)$$

$$Tr[\gamma_5 a\bar{b}c\bar{d}e] = 0 \quad (C.12)$$

$$Tr[\gamma_5 a\bar{b}c\bar{d}e\bar{f}] = 4i\varepsilon_{\alpha\beta\gamma\delta} a^\alpha b^\beta c^\gamma d^\delta \quad (C.13)$$

where

$$\varepsilon_{\alpha\beta\gamma\delta} = \begin{cases} +1 & \text{for an even permutation of } 0,1,2,3 \\ -1 & \text{for an odd permutation of } 0,1,2,3 \\ 0 & \text{if two or more indices are the same} \end{cases}$$

独创性声明

本人声明所呈交的学位论文是本人在导师指导下进行的研究工作及取得的研究成果。据我所知，除了文中特别加以标注和致谢的地方外，论文中不包含其他人已经发表或撰写过的研究成果，也不包含为获得 重庆大学 或其他教育机构的学位或证书而使用过的材料。与我一同工作的同志对本研究所做的任何贡献均已在论文中作了明确的说明并表示谢意。

学位论文作者签名：曾代敏

签字日期：2004 年 5 月 20 日

学位论文版权使用授权书

本学位论文作者完全了解 重庆大学 有关保留、使用学位论文的规定，有权保留并向国家有关部门或机构送交论文的复印件和磁盘，允许论文被查阅和借阅。本人授权 重庆大学 可以将学位论文的全部或部分内容编入有关数据库进行检索，可以采用影印、缩印或扫描等复制手段保存、汇编学位论文。

保密（），在_____年解密后适用本授权书。

本学位论文属于

不保密（）。

（请只在上述一个括号内打“√”）

学位论文作者签名：曾代敏

导师签名：王其信

签字日期：2004 年 5 月 20 日

签字日期：2004 年 5 月 20 日